福 井 大 学 審 査
学 位 論 文 [博 士 (工 学)]

Voltammetric current in viscous sodium alginate solutions

(アルギン酸ナトリウムの粘性水溶液における
ボルタンメトリー)

平成二十五年九月

王　　博

Contents

Chapter 4

Slow scan voltammetry for diffusion-controlled currents in sodium alginate solutions

Chapter 5

Abstract

Whether mass transport rates in viscous sodium alginate (SA) are dependent of viscosity is a controversial issue because few data reported on the size of network. This thesis considered the mass transport behavior of three different species in viscous SA solutions by means of voltammetry, dynamic light scattering (DLS) and time-evolution of diffusing dye. Applications were also explored in the light of its unique mass transport property.

This thesis consists of five chapters. Chapter 1 is devoted to introduction of the sodium alginate, determining of diffusion coefficient, slow scan voltammetry and cylindrical electrode. The experimental procedures are described in chapter2. Chapter 5 is the conclusions.

Chapter 3 deals with the effects of viscosity on the voltammetric current of FcTMA. Voltammograms were almost independent of the increasing viscosity of the SA solution even in a solid-like state. The diffusion coefficient of the FcTMA did not vary with the viscosity evaluated by a viscometer. Because change in redox charge may cause complications on the value of diffusion coefficients by means of electrochemical measurement, the variation of conductivity with viscosity was also measured. The conductivity was not only independent of *D* but also of redox species. The independence was confirmed by means of time-evolution of diffusing dye experiment. The result showed the *D*-values were close to the value of organic molecular in water regardless of the viscosity. The intrinsic viscosity was evaluated. The value 15 dm^3g^{-1} equivalent to the volume as large as $3m^3$ of water in which one mole of the unit of SA polymer generates the viscosity. In contrast, diffusion coefficients of the latex particle which was 0.84μm and 0.42μm in diameter by DLS and Stokes-Einstein equation respectively, decreased with the increasing of the viscosity of SA. It demonstrated molecules bigger than that volume would exhibit viscous effects by blocking diffusion with the network of SA. As an application, it can use for long long-term chronoamperometry experiments. The reproducible current of different angle of electrode surface against the horizon (0, 60) got with the time even of 1500s without any effect of nature convection, whereas it was irreproducible for times longer than 20s. Consequently, SA works as stabilization of diffusion currents by blocking the nature

convection. Because the electrodeposition of silver in aqueous often shows granular, spongy and dendritic morphology owing to the nonuniform current distributions caused by nature convection, that unique property can be used for deposition of silver. The silver film deposited in SA solution exhibited no morphology even on an optical microscopy scale.

Chapter 4 focus on the slow scan voltammetry in SA solutions. For a voltammetry experiment at a stationary, constant-area electrode, the charging current always exist since the potential is continuously changing in a potential sweep experiment. The diffusion current must always be measured from a baseline of charging current. While capacitive current is proportional to the square root of scan rate and Faradaic diffusion current varies with square root of scan rate, so that capacitive current is relatively more important at high scan rates, especially in low concentrations. Voltammetry at low scan rate has always been used for extracting Faradaic diffusion current from capacitive one in determining lower concentration solutions. It is necessary to avoid unexpected nature convection because it is a long-term experiment. The linear sweep voltammograms of two redox species, FcTMA and potassium hexacyanoferrate in KCl solution with SA at platinum disc electrode were clear , reproducible and propotional to the square root of scan rate, whereas that in aqueous solution were complicatedly wave-like variations at lower scan rate. The peak currents with SA were almost the same as those without SA, whereas they were smaller than those without SA at low scan rate. The ratio of the peak currents with SA to that without SA was increased with decreasing of scan rate. The similar variation of voltammograms and peak current happened at platinum wire electrode 0.1mm in diameter and 10mm in length, but a wire electrode were more strongly affected by natural convection than a disc electrode at low scan rate. Irreproducible and larger chronoamperometric currents at the wire electrode were noticeable earlier than that at the disk electrode. Slow scan voltammetry is suitable for detection of redox species with low concentrations. A wire electrode in SA solution was demonstrated to be a powerful tool for determining concentrations up to 0.5μM at 0.1 mV s^{-1}. The faradaic current waves were obtained clearly and reproducibly even at 0.01 mV s^{-1}.

Acknowledgments

This work was accomplished at Department of Applied Physics Graduate school of Engineering, University of Fukui under the supervision of Professor Koichi Aoki from October 2013.

Foremost, I would like to express my deepest appreciation and sincere gratitude to my supervisor Professor Koichi Aoki for his patience, motivation, enthusiasm, and immense knowledge. His guidance helped me in all the time of research and writing of this thesis. I could not have imagined having a better advisor and mentor for my study.

In addition, I would like to thank the Associated Professor Jingyuan Chen whose advices and insight was invaluable and important to me. Her attitude to research inspired me to continue to be a PhD.

My appreciation also goes to Dr. Nishiumi Toyohiko, for his opinion and suggestions during the seminar.

Thanks to all other Aoki members, especially my tutor Anma Hikaru for his enthusiasm, warmness, continuous supports and selfless assistance.

Last but not the least, I would like to thank my parents, my relatives, my elder sister, her husband and her two lovely children. Nothing can express my gratitude for their help and spiritual supporting throughout my life.

Sincerely yours:

Wang Bo

Department of Applied Physics

University of Fukui

Introduction

1.1 Sodium alginate

Alginate is a natural occurring polysaccharide extensively existed in brown algae and bacteria. Since Hirst and Rees were succeed in isolating D-mannuronic acid (M) and L-guluronic acid (G) from alginic acid, alginate was demonstrated to be a linear polymer of M and G residues linked together without branches[1]. The chemical and physical properties of alginate depend on the proportional and distribution of segments, along with their alternating sequence.

As a water-soluble polysaccharide, sodium alginate can form hydrocolloid, dispersions or gels by crosslinking with many cations. Generally, the chemical composition and the number and length of the guluronate residues determine the the affinity of alginates to ions. Calcium ion can form the so called 'egg-box' structure by interaction with GG blocks, that was also occur in MM and MG blocks by crosslinking with zinc ion[2].

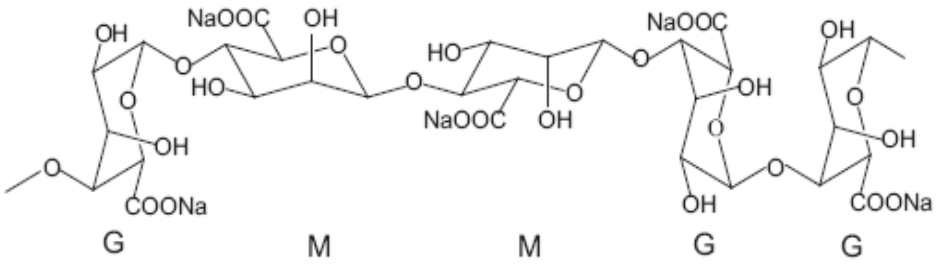

Scheme 1.1 Structure of sodium alginate

Extensive applications were explored in light of its specific properties. Such as, sodium alginate as additives in ice cream can improve smoothness of body, give uniformity of product, desired resistance to melting and hinder crystal growth. That is

probably because sodium alginate can affect the freezing properties and hinder recrystallization. Because alginate gel can be easily formed and dissolve under physiological conditions, alginate gel beads have been used as a suitable vehicle for controlling release rate of drug. A scaffolding material in tissue engineering should control cell adhesion, growth and new tissue formation in 3-*D*. sodium alginate hydrogels have been applied to tissue engineering because of their biocompatibility, abundance in source, and low prices. The direct electron transfer process of redox proteins are difficult to research at naked solid electrode due to the deep burying of the electroactive center of protein and the unfavorable orientation of the protein structure on the electrode surface. Sodium alginate has been designed for forming a biocomposite ultrathin films that can immobilize the redox protein on the electrode surface and provide a suitable microenvironment for retaining the protein structure and promote the electron transfer rate. Sodium alginate has been also applied to textile, thickeners, emulsifiers. The extensive applications lie in modifiable scaffold of functional species in films or gel under biocompatible circumstances.

In general, mass transport rates in viscous sodium alginate solutions decrease owing to the frictional resistance. For example, the detection time of oxygen at the Clark-type chip was prolonged 1.5 times when the chip contained sodium alginate [4]. The higher was the viscosity of sodium alginate, the lower was the separation sensitivity of pervaporation [3]. Some opposite data have been reported [5,4-6,7], in which mass transfer rates are independence of viscosity. The concept of the independence is based on the prediction that molecules can transfer through a large network of sodium alginate [13,15-19]. This controversial issue motivated us to research on the mass transport rates in viscous sodium alginate. Because few data reported on the size of network, this thesis considered the mass transport behavior in viscous SA solutions by means of voltammetry, dynamic light scattering (DLS) and time-evolution of diffusing dye.

1.2 Diffusion coefficient

Viscous solutions have extensive applications in electrochemical research and solid –state battery industrial. Studies on mass transport rate in viscous solution are important in understanding of ion-polyion and polyion-polyion interactions, the structure of the viscous solution, and the development of solid-state rechargeable lithium batteries.

In generally, diffusion coefficient in viscous solutions was obtained by means of measurement of steady-state diffusion current. Hydrodynamic method can obtain steady-state rather quickly with a high precision, often without the need for recorders or oscilloscopes. Moreover, charging current does not enter this measurement at steady-state. The rotating disk electrode is a useful device for which the hydrodynamic equation and convection-diffusion equation have been solved rigorously for steady state. Another available tool is the Couette-flow between two concentric cylinders. It can determine not only diffusion coefficient, but also viscosity. Transient methods which based on the measurement of transient current after a voltage step have been explored too.

Because of the poor conductance of the solution caused by retarded ion transport and limited ionic solubility, the measurements of transport rate by electrochemical methods are quite complicate. For example, the kinetics of electron transfer in polymer electrolytes is more important both practically and fundamentally. The poor conductance deforms voltammetric waves as if sluggish electrode kinetics were to be involved in reactions [10,11]. The decrease in ionic solubility enhances adsorption of redox species, e.g., ferricenium ion as an oxidation product [12]. Strong temperature-dependence of viscosity causes poor reproducibility of data. Despite these complications, some fundamental features proper to viscosity have been reported; slip effects which deviates the proportionality of shear stress to velocity [13], deviation from Levich's equation at Reynolds number less than 30 [14], inhomogeneity of redox sites in

polymer giving rise to a delay of diffusion currents [15], dependence of diffusion coefficients on concentrations of redox species [16], estimation of solvent-solute interaction [17], and deviation from the inverse proportion of diffusion coefficients to viscosity [18,19].Mass transport rates in viscous sodium alginate are controversial because of few data reported on size of the network [5]. Determination of transport properties of viscous solution can give us useful information about the structure of the solvent composition and ion-solvent interactions. Discussion of a diffusion coefficient is generally related to the Stokes-Einstein equation [20]. It has been obtained from the concept that the thermal motion of a transport particle is compensated with the viscous friction. Difference between the macroscopic viscosity obtained by a viscometer and the microscopic viscosity which the particle experiences may reflect the polymer structure of sodium alginate.

1.3 Slow scan voltammetry

For a voltammetry experiment at a stationary, constant-area electrode, the charging current always exist since the potential is continuously changing in a potential sweep experiment. The diffusion current must always be measured from a baseline of charging current. While capacitive current is proportional to the square root of scan rate and Faradaic diffusion current varies with square root of scan rate, so that capacitive current is relatively more important at high scan rates, especially in low concentrations. Voltammetry at low scan rate has always been used for extracting Faradaic diffusion current from capacitive one in determining lower concentration solutions. It is necessary to avoid unexpected nature convection because it is a long-term experiment.

As we known, the graphite and graphitized carbon materials are considered as excellent anodes for high-energy density Li^+ insertion rechargeable batteries. Formation of effective passivation layers may result in high reversibility of the subsequent Li^+

intercalation reaction. The Li-graphite intercalation mechanism was studied by using classical cyclic vlotammmetry. Studies of diffusion coefficient provided more useful information about the entire intercalation mechanism. Slow scan rate allowed us to estimate the effective heterogeneous rate constant [21]. The voltammetric peak currents were controlled by diffusion of lithium in graphite, as was demonstrated by the proportionality of the currents to square-roots of scan rates [21].The controlling step was also supported by the Cottrell plot for long-term chronoamperometric responses of reduction of lithium ions [22]. The voltammetric capacitive current is, in contrast, proportional to the scan rate. If observed current is a simple sum of the diffusion-controlled current, I_d, and the capacitive one, I_c, the ratio, I_c/I_d, decreases by 10 times with 100 times decrease in the scan rates. This is the advantage of extremely slow scan voltammetry. A long term measurement can get reproducible voltammograms by preventing disturbance from natural convection. Fortunately, the current by the intercalation is controlled by diffusion of metal atoms into solid anodes [21,23-25] and solid cathodes [26-29], and hence disturbance by convection ought to be suppressed. This advantage has been realized also in voltammetry at film-coated electrodes in a thin layer cell [30-36].Slow scan voltammetry has also been applied to detection of catalytic currents [37-41] at the aim of enhancing catalytic kinetics over mass transport. It has been used for obtaining well-defined voltammograms at low temperatures [42].

Viscous solvents are a good technique for suppressing natural convection [43-51]. An increase in the viscosity decreases generally the diffusion coefficient, according to the Stokes-Einstein equation [52], so that Faradaic currents also decrease. Addition of sodium alginate (SA) enhances the viscosity without changing diffusion coefficients of molecules [44,46,53-56]. Molecules may not collide with the network of SA but diffuse through the domain of the aqueous solution [56]. Consequently slow scan voltammetry in SA may exhibit a potentiality of extracting Faradaic currents from capacitive ones.

1.4 Cylindrical electrode

The cylindrical electrode is simple to construct and consists of a metal wire or a carbon fiber sealed in insulating material, for example, glass or resin. Thin cylindrical electrode has attracted extensive attention due to the application of electrochemical in vivo measurement. In vivo measurement can provide direct, continuous, and in situ information without sample preparation. Biosensor is one of the successful applications of cylindrical electrode for detection of biological material in situ.

A long cylindrical or a long wire electrode can be used for detection of low concentrations because long wire electrode can supply large current under quasi steady-state current [57,58]. A wire electrode has another advantage of yielding reproducible Faradaic currents, because the boundary between the wire and the insulator which often causes floating capacitive currents is much shorter than the length of the wire [59,60]. In sodium alginate solutions, the polymer backbones and their entanglement may work as maintaining high viscosity. A sensitive Faradaic current without the effect of natural convection might be available at slow scan rates. Another technique for extracting Faradaic currents is microelectrode voltammetry. Unfortunately, microdisk electrodes are unsuitable for detecting low concentrations because the current is very small. Microdisk array electrodes and microband electrodes have large surface area. However, they also have long boundaries between the electrode and the insulating wall, which yields large irreproducible capacitive current.

1.5 Aim of this thesis

Sodium alginate has extensive applications lie in modifiable scaffold of function species in film or in gel. Whether mass transport rates in viscous sodium alginate (SA) are dependent of viscosity is a controversial issue. So we paid attention to the relationship between diffusion coefficients of FcTMA in different concentration of

sodium alginate solutions. The size of network may play a important role in this relationship. So mass transport rate of latex in sodium alginate was also measured by DLS. The size of the network should was calculated by intrinsic viscosity. As a viscous solution, Sodium alginate solutions were predicted to be useful to keep ideal concentration profile. This unique property may be applied to long-term chronoamperometry experiment, the electrodeposition of silver and slow scan voltammetry for measurement of low concentrations. The main issues in this thesis contain: (1) The dependent of diffusion coefficients in different viscosity of sodium alginate solutions; (2) The size of the network; (3) The performance of viscous sodium alginate solutions in long-term chronoamperometry experiment, the electrodeposition of silver and slow scan voltammetry in low concentration solutions.

1.6 References

[1] A. Haug, B. Larsen, O. Smidsrod, Acta Chem. Scand. 20 (1966) 183.

[2] P. Aslani, R.A. Kennedy, Journal of Controlled Release 42 (2006) 75.

[3] U.S. Toti, T.M. Aminabhavi, J. Membr. Sci. 228 (2004) 199.

[4] M. Grassi, I. Colombo, R. Lapasin, J. Control. Rel. 76 (2001) 93.

[5] W. Lubas, P. Ander, Macromolecules 13 (1980) 318.

[6] Y. Li, X. Zhao, Q. Xu, Q. Zhang, D. Chen, Langmuir 27 (2011) 6458.

[7] A. Mohanan, B. Vishalakshi, Int. J. Polym. Mat. 58 (2009) 561.

[8] A.R. Kulkarni, K.S. Soppimath, T.M. Aminabhavi, W.E. Rudzinski, Eur. J. Pharm. Biopharm. 51 (2001) 127.

[9] D. Şolpan, M. Torun, J. Appl. Polym. Sci. 100(2006) 335.

[10] H. Zhou, S. Dong, Electrochim. Acta 42 (1997) 1801.

[11] H. Zhou, N. Gu, S. Dong, J. Electroanal. Chem. 441 (1998) 153.

[12] I. Svorstøl, T. Sigvartsen, J. Songstad, J. Acta Chem. Scand. B42 (1988) 133.

[13] R.A. Mashelkar, A. Dutta, Chem. Eng. Sci. 37 (1982) 969.

[14] J. Legrand, E. Dumont, J. Comiti, F. Fayolle, Electrochim. Acta 45 (2000) 1791.

[15] K. Aoki, K. Tokuda, H. Matsuda, N. Oyama, J. Electroanal. Chem. 176 (1984) 139.

[16] P. Daum, J. R. Lenhard, D. Rolison, R. W. Murray, J. Am. Chem. Soc. 102 (1980) 4649.

[17] P. Zuman, D. Rozbroj, J. Ludvík, M. Aleksic, L. Camaione, H. Celik, J. Electroanal. Chem. 553 (2003) 135.

[18] K. Aoki, Y. Guo, J. Chen, J. Electroanal. Chem. 629 (2009) 73.

[19] Y. Guo, K. Aoki, J. Chen, T. Nishiumi, Electrochem. Acta, 56 (2011) 3727.

[20] P.W. Atkins, Physical Chemistry, Sixth edition, Oxford University Press, Oxford, 1998, p. 479

[21] M.D. Levi, D. Aurbach, J. Electroanal. Chem. 421 (1997) 79.

[22] M.D. Levi, E.A. Levi, D. Aurbach, J. Electroanal. Chem. 421 (1997) 89.

[23] M. Minakshi, Electrochim. Acta 55 (2010) 9174.

[24] T. Ohzuku, Y. Iwakoshi, K. Sawai J. Electrochem. Soc. 140 (1993) 2490.

[25] F. Nobili, S. Dsoke, M. Mancini, R. Tossici, R. Marassi, J. Power Sources 180 (2008) 845.

[26] J.-H. Kim, K. Zhu, J. Y. Kim, A. J. Frank, Electrochim. Acta 88 (2013) 123.

[27] Z. Lu, M.D. Levi, G. Salitra, Y. Gofer, E. Levi, D. Aurbach, J. Electroanal. Chem. 491 (2000) 211.

[28] M. Liberatore, F. Decker, A. S. Vuk, B. Orel, G. Drazic, Solar Energy Mat. 90 (2006) 434.

[29] K.M. Begam, Y.H. Taufiq-Yap, M.S. Michael, S.R.S. Prabaharan, Solid State Ionics 172 (2004) 47.

[30] C. Shi, F. C. Anson, Anal. Chem. 70 (1998) 3114.

[31] C. Shi, F. C. Anson, J. Phys. Chem. B 103 (1999) 6283.

[32] M. Liberatore, A. Petrocco, F. Caprioli, C. La Mesa, F. Decker, C.A. Bignozzi, Electrochim. Acta 55 (2010) 4025.

[33] T.D. Chung, J. Kor. Electrochem. Soc. 5 (2002) 216.

[34] F. Quentel, V. Mirceski, M. L'Her, F. Spasovski, M. Gacina, Electrochem. Commn. 9 (2007) 2489.

[35] V. Mirceski, R. Gulaboski, I. Bogeski, M. Hoth, J. Phys. Chem. C 111 (200) 6068.

[36] X. Liu, L. Hu, L. Zhang, H. Liu, X. Lu, Electrochim. Acta 51 (2005) 467.

[37] F. Maillard, M. Martin, F. Gloaguen, J.-M. Leger, Electrochim. Acta 47 (2002) 3431.

[38] Y. Liu, S. Mitsushima, K. Ota, N. Kamiya, Electrochim. Acta 51 (2006) 6503.

[39] F. Seland, R. Tunold, D. A. Harrington, Electrochim. Acta 55 (2010) 3384.

[40] M. Yagi, K. Nagai, T. Onikubo, M. Kaneko, J. Electroanal. Chem. 383 (1995) 61.

[41] A.D. Modestov, M.R. Tarasevich, H. Pu, J. Power Sources 205 (2012) 207.

[42] M. Opallo, J. Electroanal. Chem. 411 (1996) 145.

[43] C.-C. Wu, H.-N. Luk, Y.-T. T. Lin, C.-Y. Yuan, Talanta 81 (2010) 228.

[44] A. Kikuchi, M. Kawabuchi, A. Watanabe, M. Sugihara, Y. Sakurai, T. Okano, J. Control. Rel. 58 (1999) 21.

[45] G. Zhao, X. Zhan, W. Dou, Anal. Biochem. 408 (2011) 53.

[46] A.C.F. Ribeiro, A.J.F.N. Sobral, S.M.N. Simoes, M.C.F. Barros, V.M.M. Lobo, A. M.T.D.P.V. Cabral, F.J.B. Veiga, C.I.A.V. Santos, M.A. Esteso, Food Chem. 125 (2011) 1213.

[47] K. Aoki, Y. Guo, J. Chen, J. Electroanal. Chem, 629 (2009) 73.

[48] Y. Guo, K. Aoki, J. Chen, T. Nishiumi, Electrochem. Acta, 56 (2011) 3727.

[49] J. Legrand, E. Dumont, J. Comiti, F. Fayolle, Electrochim. Acta 45 (2000) 1791.

[50] R. D. Tonini, M. R. Remorino, F. M. Brea, Electrochim. Acta, 23 (1978) 699.

[51] J. van der Gucht, N. A. M. Besseling, H. P. van Leeuwen, J. Phys. Chem. B 108 (2004) 2531.

[52] P.W. Atkins, Physical Chemistry, Sixth edition, Oxford University Press, Oxford, 1998, pp. 690.

[53] M. Grassi, I. Colombo, R. Lapasin, J. Control. Rel. 76 (2001) 93.

[54] W. Lubas, P. Ander, Macromolecules 13 (1980) 318.

[55] Y. Li, X. Zhao, Q. Xu, Q. Zhang, D. Chen, Langmuir 27 (2011) 6458.

[56] K. Aoki, B. Wang, J. Chen, T. Nishiumi, Electrochim. Acta, 83 (2012) 348.

[57] K. Aoki, K. Honda, K. Tokuda, H. Matsuda, J. Electroanal. Chem. 182 (1985) 267.

[58] K. Aoki, Electroanalysis 5 (1993) 627.

[59] K. Aoki, Y. Hou, J. Chen, T. Nishiumi, J. Electroanal. Chem. 689 (2013) 124.

[60] K. Aoki, X. Zhao, J. Chen, T. Nishiumi, J. Electroanal. Chem. 697(2013)5.

Experimental

2.1 Chemicals

Powder of sodium alginate (Wako), of which molecular weight corresponded to 500-600 mPa s in 10 g dm^{-3} solution, was used as received. It was stored in a refrigerator. The electroactive species, ferrocenyl tetramethylammmonium hexafluorophosphate (FcTMA), was synthesized in house. FcTMA contained salt, mainly ammonium iodide, which was formed when iodide in ferrocenyl tetramethylammmonium iodide was substituted for hexafluorophosphate. Water was deionized and distilled. Polystyrene latex was synthesized in house[1]. Potassium hexacyanoferrate (Ⅲ) was of analytical grade (Wako).

2.2 Instruments and processes

A homogeneous solution of sodium alginate was prepared by dissolving sodium alginate powder in distilled water at 60^{o}C and mixing slowly. Viscous solution contained air bubbles coming from the powder. Bubbles were removed by ultrasonication for 30 min. Mixing of very viscous solution was made by squeezing the mixture in a polyethylene bag.

Accurate concentrations of FcTMA solution were determined by the combinational use of voltammetric peak currents at the platinum electrodes 1.6 mm and 0.1 mm in diameters[2]. This technique included the following steps; carrying out voltammetry at the two electrodes for the potential scan rates, v, in the range from 10 to 100 mV s^{-1}, evaluating the proportionality constant of the peak current, I_p, vs. $v^{1/2}$ at the 1.6 mm electrode, evaluating the extrapolated limiting current, I_L, to $v^{1/2} \rightarrow 0$ at the 0.1 mm electrode in the I_L', vs. $v^{1/2}$ plot, and taking the ratio of the $(I_p v^{-1/2})^2/I_L$. In contrast the ratio $(I_p v^{-1/2})/I_L$ provided values of the diffusion coefficient of FcTMA without knowing

accurate concentrations.

Uniformity of size of the latex in aqueous suspension was confirmed by an optical microscope, VH-5000 (Keyence, Osaka). The size distribution of latex particles was determined by a dynamic light scattering (DLS) instrument (Malvern Zetasizer Nano-ZS, UK). Diameters by a scanning microscope and DLS were identical within experimental errors.

A conductometer was home-made by arranging two platinum disk electrodes flush with a polytetrafluoroethylene plate. The separation of two electrodes was 5.5 mm. Alternating voltage with 1 kHz and 10 mV amplitude was applied to the electrodes. The in-phase component of the responding current was collected through a potentiostat. It was calibrated with several concentrations of KCl solution ranging from 0.01 to 0.1 M to determine the cell constant.

Cyclic voltammetry was carried out with a potentiostat, Compactstat (Ivium Tech., Netherlands), in viscous mixtures. Platinum wire 0.1 mm in diameter, Platinum disks 1.6 mm and 0.1 mm in diameter (BAS, Tokyo) were used as voltammetric working electrodes. The surface of the working electrode was polished with alumina paste on wet cotton, and was rinsed with distilled water in an ultrasonic bath.

Viscosity was determined with a vibration viscometer, SV-10 (A&D, Tokyo), at room temperature after each voltammetric measurement. Viscosity was also obtained under the temperature control from 0 to 73^{o}C

2.3 References

[1] H. Chen, J. Chen, K. Aoki, T. Nishiumi, Electrochim. Acta, 53 (2008) 7100.

[2] H. Zhang, K. Aoki, J. Chen, T. Nishiumi, H. Toda, E. Torita, Electroanalysis 23 (2011) 947.

Diffusion coefficients in viscous sodium alginate solutions

3.1 Aim

Sodium alginate is a water-soluble, natural occurring linear polysaccharide [1,2]. It takes a form of viscous hydrocolloid, dispersions or gels by crosslinking. It has been widely applied to safety food additives, pharmaceutical materials, textile, thickeners, emulsifiers, and stabilizers [3]. The extensive applications lie in modifiable scaffold of functional species in films or gel [4-7] under biocompatible circumstances [6,8-11]. Viscous sodium alginate solutions decrease in general mass transfer rates owing to the frictional resistance. For example, the detection time of oxygen at the Clark-type chip was prolonged 1.5 times when the chip contained sodium alginate [4]. The higher was the viscosity of sodium alginate, the lower was the separation sensitivity of pervaporation [12]. Some opposite data have been reported [5,7,13-15], in which mass transfer rates are independence of viscosity. The concept of the independence is based on the prediction that molecules can transfer through a large network of sodium alginate [13,15-18].

Electrochemical measurements in viscous solutions are complicated by poor conductance of solution due not only to retarded ion transport but also to limited ionic solubility. The poor conductance deforms voltammetric waves as if sluggish electrode kinetics were to be involved in reactions [19,20]. The decrease in ionic solubility enhances adsorption of redox species, e.g., ferricenium ion as an oxidation product [21]. Strong temperature-dependence of viscosity causes poor reproducibility of data. Despite these complications, some fundamental features proper to viscosity have been reported; slip effects which deviates the proportionality of shear stress to velocity [22], deviation from Levich's equation at Reynolds number less than 30 [23], inhomogeneity of redox sites in polymer giving rise to a delay of diffusion currents [24], dependence of diffusion coefficients on concentrations of redox species [25], estimation of

solvent-solute interaction [26], and deviation from the inverse proportion of diffusion coefficients to viscosity [27,28].

Mass transport rates in viscous sodium alginate are controversial because of few data reported on size of the network [5]. The data required for the discussion are a diffusion coefficient, D, and viscosity, η, which are generally related through the Stokes-Einstein equation [29]

$$D = k_B T/6\pi\eta r_0 \qquad (3.1)$$

where r_0 is the hydrodynamic radius of spherical diffusing particle, and k_B is the Boltzmann constant. Eq. (3.1) has been obtained from the concept that thermal motion of a particle is compensated with the viscous friction. If the macroscopic viscosity obtained by a viscometer is different from the microscopic viscosity which the particle experiences, Eq. (3.1) does not hold. Difference between the two viscosities may reflect polymer structure of sodium alginate. This work is devoted to examining Eq. (3.1) in sodium alginate solutions containing a redox species by combining voltammetry and measurements of viscosity.

3.2 Results and Discussion

3.2.1 Relation of diffusion coefficient with viscosity

Voltammetry of FcTMA was made in solutions including 0.1 M KCl and several concentrations of sodium alginate. Figure 3.1 shows voltammograms (a) without and (b) with sodium alginate at Pt electrodes (A) 1.6 mm and (B) 0.1 mm in diameter. The voltammograms in (A) at an ordinary sized electrode showed peaked shape, whereas those in (B) at a microelectrode-like small electrode exhibited steady-state like shape. The sodium alginate solution for (b) was almost in such a solid state that the solution|air boundary did not move when the boundary was turned vertically to the gravity. With an increase in concentrations of sodium alginate, voltammograms were slightly shifted in

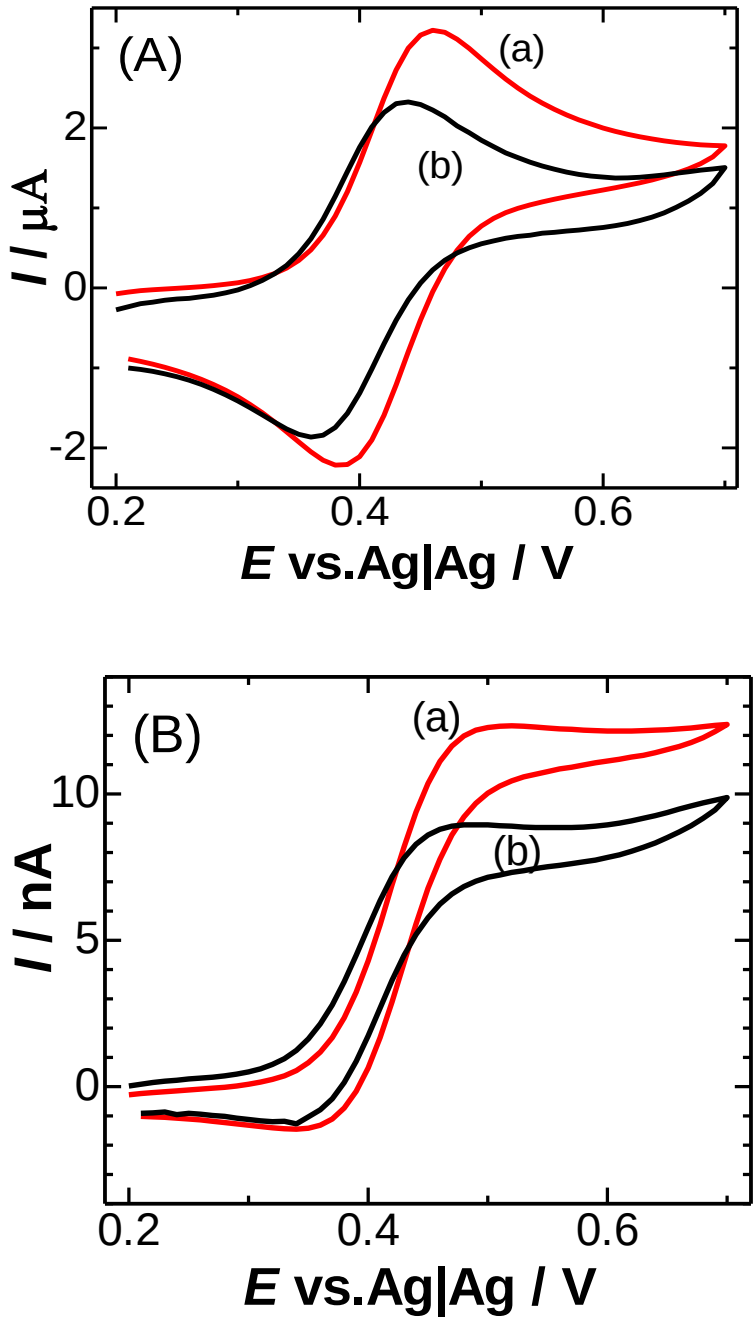

Fig. 3.1 Voltammograms of FcTMA at v = 0.1 V s^{-1} in (a) 0.1 M KCl aqueous solution and (b) sodium alginate solution with concentration of 100 g dm^{-3} at the platinum electrode (A) 1.6 mm and (B) 0.1 mm in diameter. Concentration of FcTMA was prepared to be 1 mM.

the negative direction. The maximum shift was 20 mV, as is shown in Fig. 3.1. The shift may be caused by stabilization of the reduced ferrocenyl moiety, $Fe^{2+}(C_5H_5)^-(C_5H_4\text{-})^-$, with the hydrophobic backbone of sodium alginate. Values of the peak currents at similar concentration of FcTMA in Fig. 3.1(A) did not vary largely with the viscosity although viscosity was quite different in (a) and (b). Voltammetric peak currents controlled by diffusion at an ordinary sized electrode are proportional to square-roots of the scan rate, v, whereas those at a ultramicroelectrode do not vary with v. Figure3. 2 shows variations of the peak currents with $v^{1/2}$ at the electrodes (A) 1.6 mm and (B) 0.1 mm in diameter. The former variations exhibited the proportionality, while the latter variations were not constant but increased linearly with $v^{1/2}$.

Thus, voltammograms at the 0.1 mm electrode show the intermediate property at a large electrode and at a microelectrode. A measure of the peaked current or the steady-state current is the variable $p^2 = a^2Fv/RTD$ [30], where D is the diffusion coefficient of an electroactive species. This variation should also be observed when the

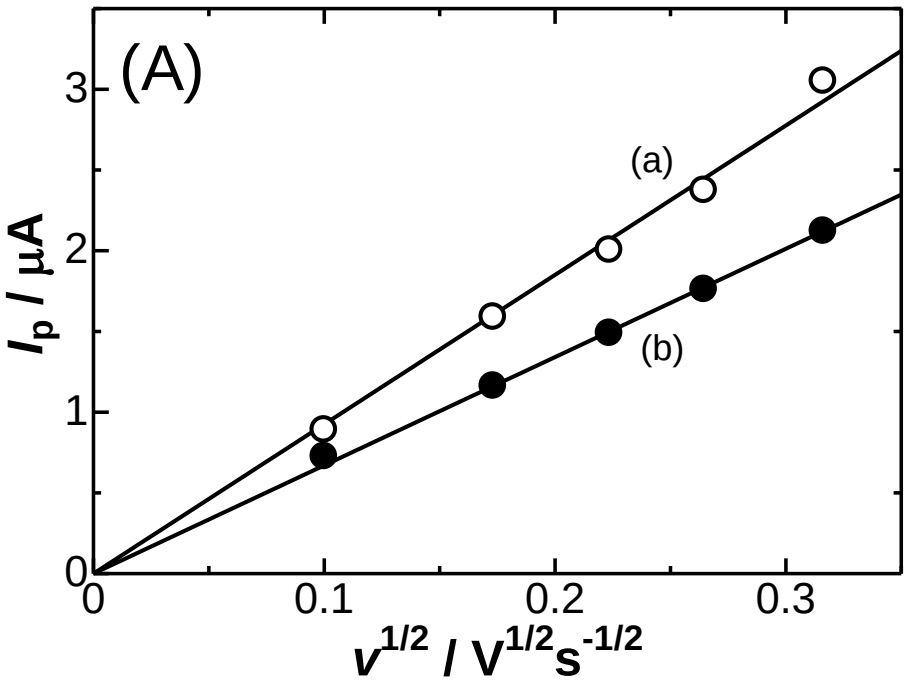

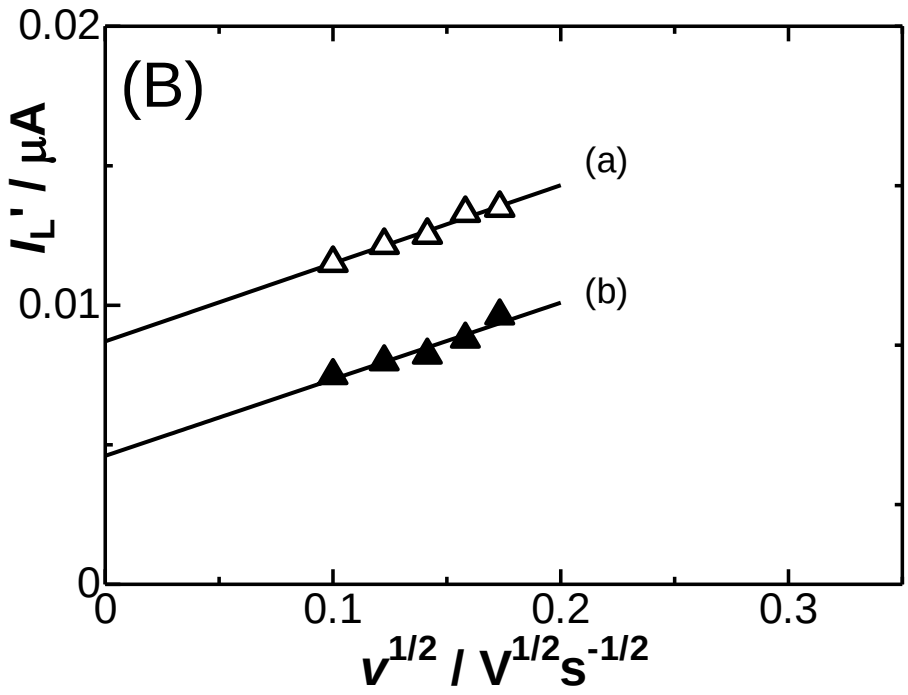

Fig. 3.2. Plots of the peak currents, I_p, (A) at the 1.6 mm disk electrode and the limiting current, I_L', (B) at the 0.1 mm disk electrode against the square-roots of the scan rate, v for ca. 1 mM FcTMA in (a) 0.1 M KCl and (b) sodium alginate solution with concentration of 100 g dm^{-3}.

diffusion coefficient becomes small in viscous media [19]. However, the voltammetric shape at the electrode 0.1 mm in diameter (Fig.3.1 B(a)) was independent of viscosity. If a value of D were to get small in the sodium alginate solution, the plot for (b) in Fig.3.2(B) should show a slope steeper than that for (a). Consequently, viscosity of sodium alginate seems to have qualitatively no effect on diffusion coefficients of FcTMA.

Evaluation of diffusion coefficients from voltammetric currents needs accurate values of concentrations. Unfortunately, it is not easy to control concentrations of FcTMA in viscous solutions because of no confirmed evidence of uniform mixing, as

can be seen from the difference in current values between (a) and (b) in Fig. 3.1 and 3.2. We determined diffusion coefficients of FcTMA by taking the ratio of the peak currents at the electrode 1.6 mm in diameter to that at 0.1 mm without knowing concentrations of FcTMA, as was presented in the experimental section. Immediately after voltammetry, viscosity was determined with the viscometer. Figure 3.3 shows the variation of the diffusion coefficient with the viscosity, η, in logarithmic axes. Values of D did not vary with η. The Stokes-Einstein equation (Eq. (1)) mentions that the slope of the plot of log(D) vs. log(η) is -1 (dotted line in Fig. (3)). Disagreement of the experimental data with Eq. (1) indicates that the viscosity experienced by the FcTMA molecule should be smaller than that by the viscometer. The data points are rather scattered at high viscosity, because of possibility of inhomogeneous mixing or fluctuation of temperature.

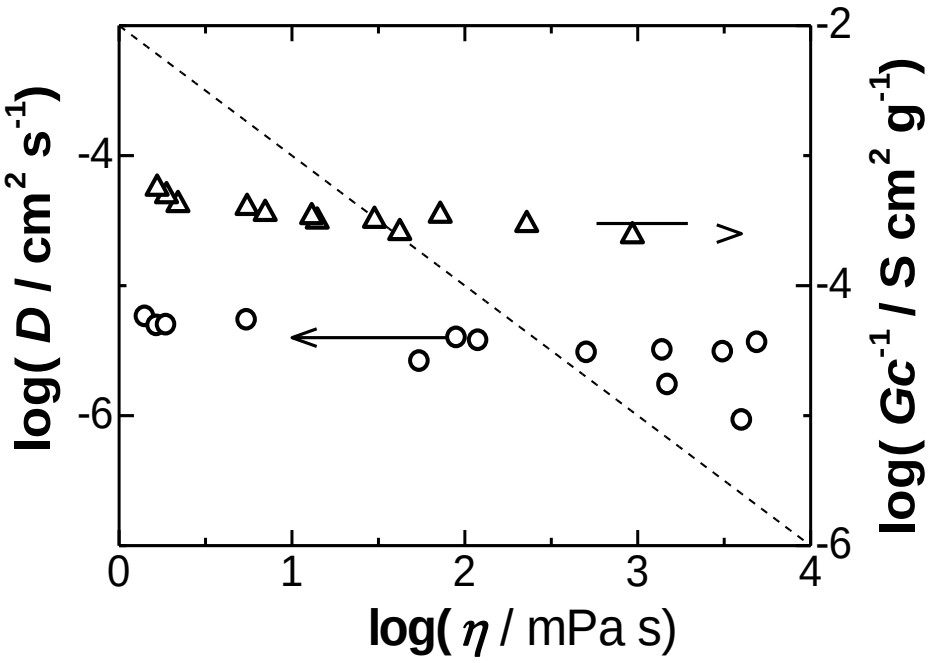

Fig.3.3 Dependence of (circles) diffusion coefficients of FcTMA and (triangles) conductance of sodium alginate on the viscosity.

The variation of the viscosity with temperature, as is shown in Fig.3.4, is much smaller than the variation in Fig. 3.3 Therefore the scattering is ascribed to insufficient mixing.

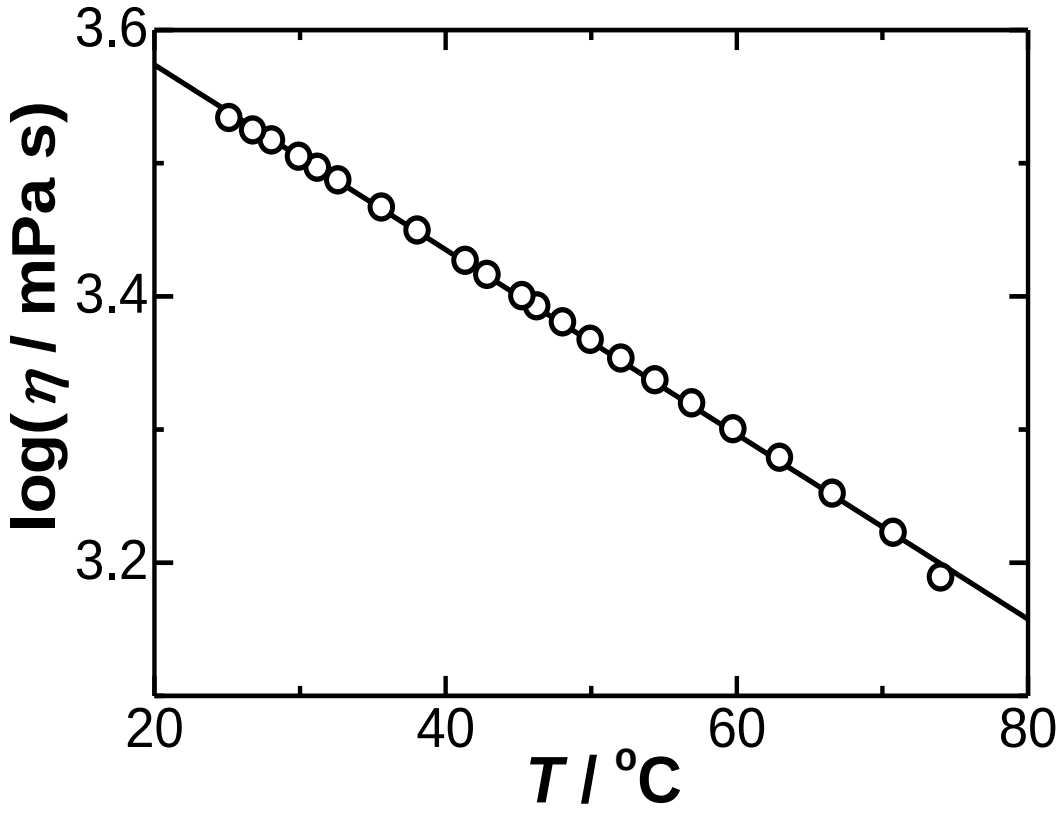

Fig.3.4. Temperature variation of viscosity of sodium alginate with concentration of 38 g dm^{-3}.

Figure 3.5 shows temperature-variations of the viscosity of sodium alginate and the diffusion coefficient of FcTMA. With an increase in the temperature, the viscosity decreased and the diffusion coefficient increased. According to the Stokes-Einstein equation, the product, $D\eta$, should increase slightly with temperature. However, it decreased because the diffusion coefficient was less influenced by temperature than the

viscosity was.

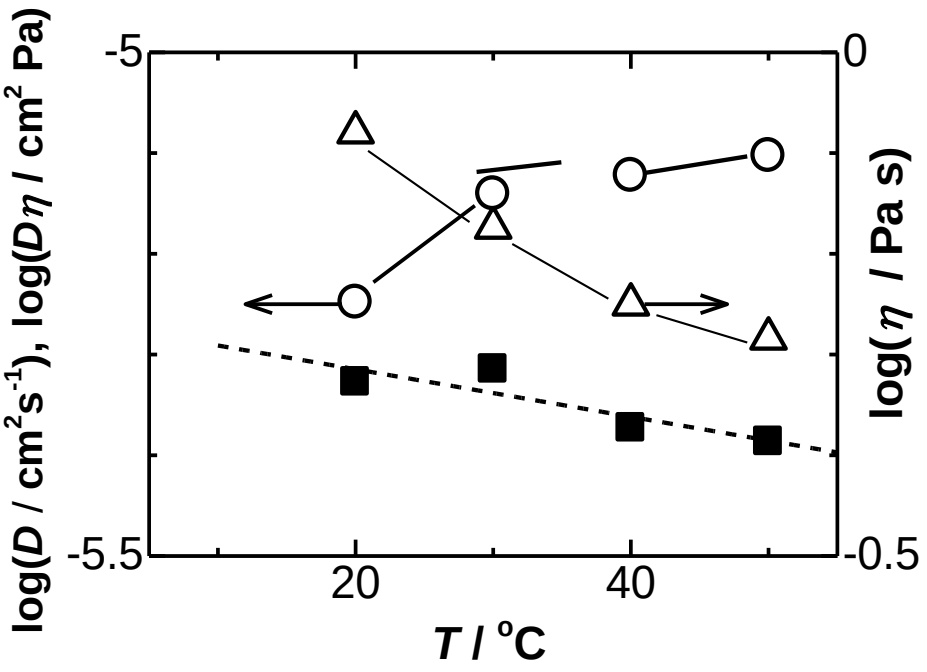

Fig.3.5. Dependence of (circles) the diffusion coefficients of FcTMA, (triangles) the viscosity of 20 g dm^{-3} sodium alginate solution and (squares) $D\eta$ on temperature.

Values of diffusion coefficients by electrochemical measurements necessarily include complications due to change in redox charge. Therefore, the invariance of D to η in Fig. 3.3 does not always come from a simple hydrodynamic effect. As an example of variation of diffusion coefficients without change in ionic charge, we paid attention to ionic conductance, which is proportional to the diffusion coefficient [29]. Conductance of Na^+ in sodium alginate was determined with the home-made calibrated conductometer in various concentrations of sodium alginate. Variation of conductivity, κ, vs. the viscosity is shown in Fig. 3.3 on the right axis. The variation was similar to that of D vs. η for FcTMA. Therefore the independence of D from η is not relevant to redox species, but is a property of sodium alginate.

The invariance of D with η might be caused by voltammetric unknown problems in viscous solutions. In order to confirm the invariance, we estimated approximate values of D in sodium alginate by use of time-evolution of diffusing dye in the following way. A viscous solution of sodium alginate was prepared on a petri dish, onto which a small amount of methylene blue-included aqueous solution was dropped. The methylene blue zone was expanded concentrically on the sodium alginate surface, as shown in Fig. 3.6.

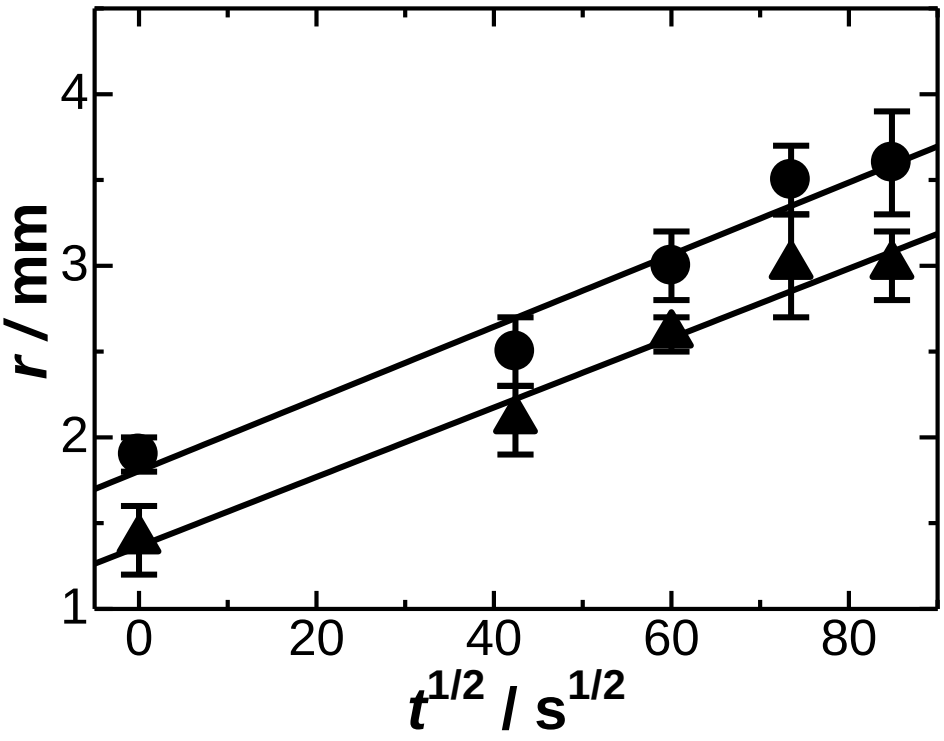

Fig. 3.6 Photographs of dispersed methylene blue drops on the sodium alginate solution with (A) 6030 and (B) 386 mPa s.

Although the boundary of the zone was not well-defined, we read outer and inner diameters of the blue circle zone at some periods after the drop. Figure 3.7 shows variations of the radii with the square-root of the time, on the concept of the thickness of a diffusion layer approximately given by $r = (Dt)^{1/2}$. As predicted, the radii had linear

variations with $t^{1/2}$. The slope provided $D = 0.5\times10^{-5}$ cm^2 s^{-1}, being common for two viscosity values (6030 and 386 mPa s). This value is not only independent on the viscosity of sodium alginate but also is close to *D*-values of organic molecules in water.

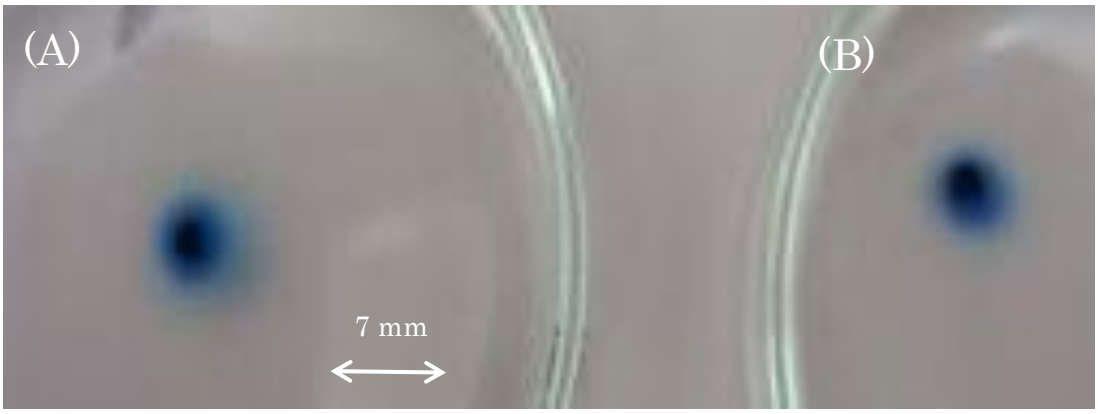

Fig.3.7 Dependence of the radii of expanded zone of the methylene blue drop on sodium alginate surface with (A) 6030 and (B) 386 mPa s on the square-roots of the time.

In order to grasp a molecular image of the independence, we discuss intrinsic viscosity [31] here. We measured the viscosity at several low concentrations of sodium alginate solutions, *c*. The viscosity increased with the concentration. Letting the viscosity of water be η^*, we obtained a linear relation of $(\eta/\eta^* - 1)/c$ with *c*, as is shown in Fig.3. 8. The intercept is the intrinsic viscosity, $[\eta] = 15$ dm^3 g^{-1}. Multiplying $[\eta]$ by the molecular weight (198 g/mol) of the unit of sodium alginate ($NaC_6H_7O_6$) yields the volume, 3.0 m^3, for the viscosity per unit of sodium alginate. This volume contains 1.7×10^5 moles of water, whereas it does one molecule of a unit of sodium alginate. Consequently, a conventional molecule such as FcTMA diffuses through water portion without colliding with the network of sodium alginate.

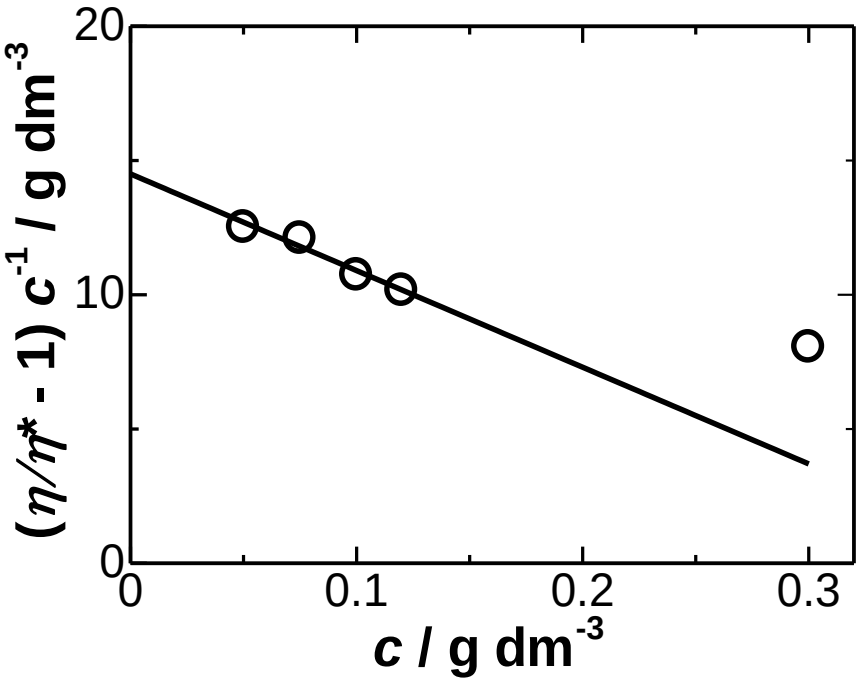

Fig. 3.8 Plot of (η/η^*-1)/c against c for low concentrations of sodium alginate.

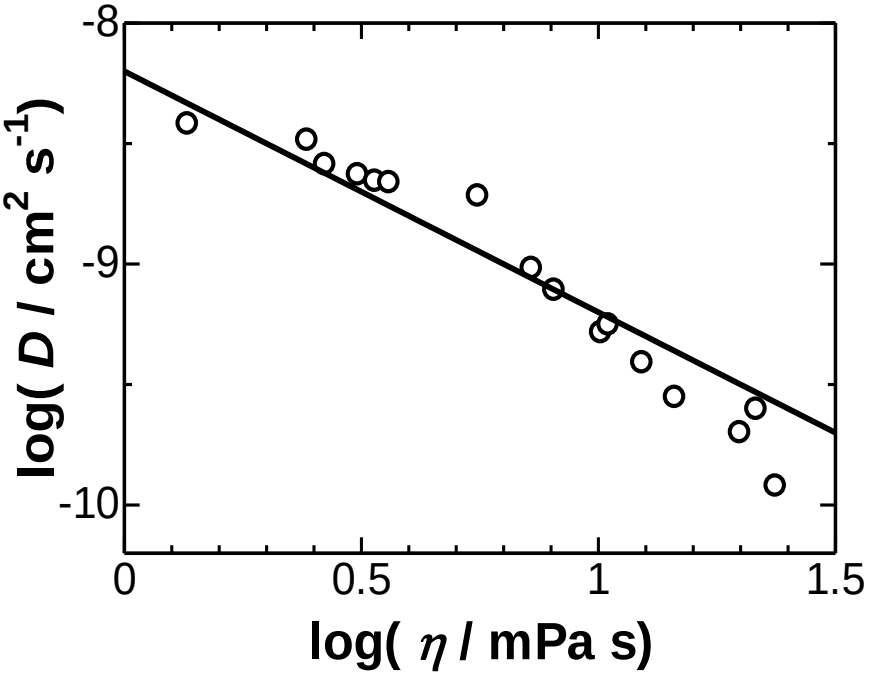

Fig.3.9 Variation of the diffusion coefficients of the latex particle with viscosity of sodium alginate. The slope of the line is -1.

Molecules bigger than this volume should exhibit viscous effects by blocking diffusion with the network of sodium alginate. This prediction was examined by dependence of diffusion coefficients of polystyrene latex particles 0.84 μm in diameter on viscosity of sodium alginate. The diffusion coefficients were estimated with DLS for a given viscosity value. Their values were decreased with an increase in the viscosity, as is shown in Fig. 3.9. They are close to the linearity (solid line) by the Stokes-Einstein equation for r_0 = 0.42 μm.

3.2.2 Applications

Long-term chronoamperometry often provides irreproducible currents owing to the buildup of density gradients and stray vibrations [32]. Currents for times longer than 30 s include convective effects, and those for times longer than 300 s are not controlled by diffusion any more [33]. Viscous sodium alginate is predicted to suppress natural convention. Figure 3.10 shows chronoamperometric curves of FcTMA in (a) 1 M KCl in viscous sodium alginate solution and (b) 1 M KCl aqueous solution. The currents in the alginate solution were decayed smoothly and were reproducible. They did not vary with angles of the electrode surface against the horizon ((i) 0 degree or (ii) 60 degree). In contrast, the currents in the aqueous solution for times longer than 100 s were irreproducible and larger than those in the sodium alginate solution. They include convection effects. Consequently, sodium alginate works as stabilization of diffusion currents by preventing convection.

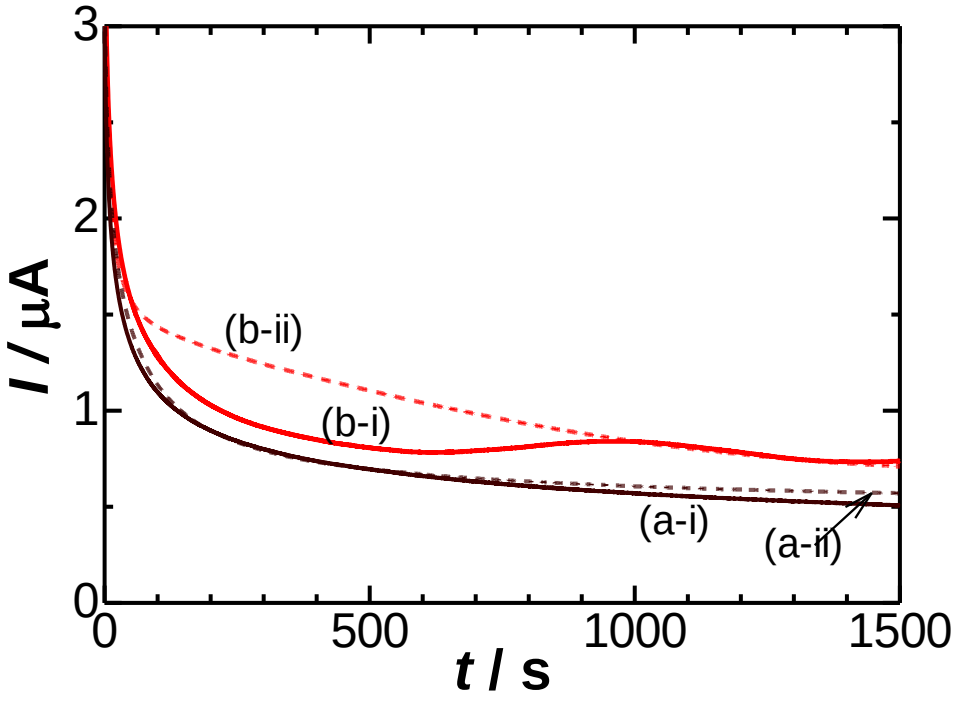

Fig.3.10. Long time chronoamperometric curves of 1 mM FcTMA in (a) 1M KCl + 25.5 g dm^{-3} sodium alginate at η = 1.34 Pa s and (b) 1 M KCl solution when 0.6 V was applied to the glassy carbon electrode 3 mm in diameter. The surface of the GC electrode in 3 mm in diameter was (i) horizontal and (ii) slanted by 60 degree.

The property of uniformizing current distributions may be applied to formation of electroplating films. Figure 3.11 shows voltammograms of silver ions (a) with and (b) without of sodium alginate. Both voltammetric shapes were similar but the current values in sodium alginate were smaller than those in solutions without sodium alginate at the identical concentration of Ag^+. The difference in values of the cathodic current does not seem to be consistent with the result in Fig.3. 1. Since sodium alginate includes carboxylic moiety, silver ion forms silver carboxylate complexes. Consequently the net concentration of silver ion to be deposited is decreased in the bulk by chelate. The charge of the reduction current in the sodium alginate solution (Fig.3. 11(a)) was close to that for a half concentration of Ag^+ (12.5 mM $AgNO_3$) in KNO_3 without sodium

alginate. Therefore a half Ag^+ was stabilized with sodium alginate.

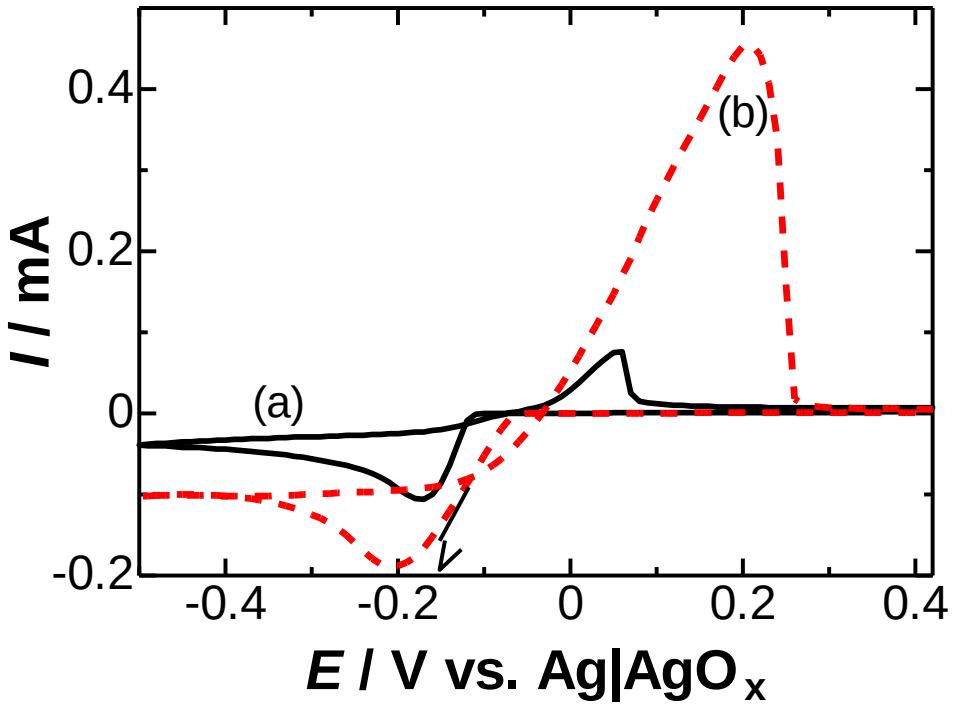

Fig.3.11. Voltammograms of 25 mM $AgNO_3$ in 1 M KNO_3 solutions (a) with and (b) without sodium alginate of 9 g dm^{-3} at the Pt electrode for v = 50 mV s^{-1}.

Silver ion was deposited on the Pt electrode at -0.3 V in 25 mM $AgNO_3$ + 1 M KNO_3 solution and in 25 mM $AgNO_3$ + 1 M KNO_3 + 9 g dm^{-3} sodium alginate solution, respectively, for 15 s and 60 s so that the cathodic charge was common (ca. 1.5 mC). The electrode was rinsed gently with water, and was observed by the optical microscope, as shown in Fig. 3.12. The photograph without sodium alginate shows a pattern (B), whereas that with sodium alginate has little morphology (A). The former is composed of basically two types of morphology; grains less than 10 μm, and domains larger than 0.1 mm. When the effective concentration of Ag^+, that is, a half the concentration was used

for deposition without sodium alginate, the deposit surface (Fig.3.12(C)) was similar to the pattern in Fig. 3.12(B). The SEM photograph (Fig. 3.13(B)) without sodium alginate shows fish-shaped grains with various sizes, whereas that (Fig. 3.13(A)) with sodium alginate exhibits no pattern. The difference is ascribed to the chronoamperometric result (Fig. 3.10) that sodium alginate prevents natural convection of silver ion.

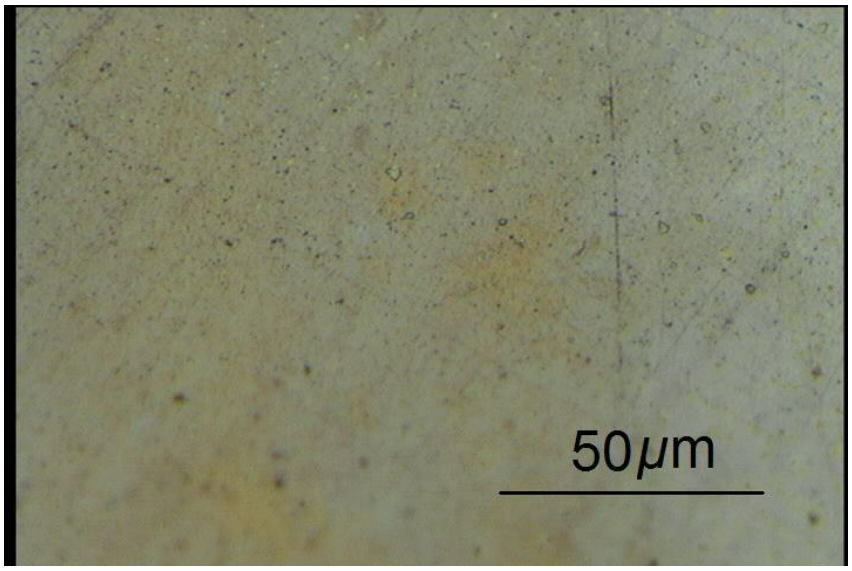

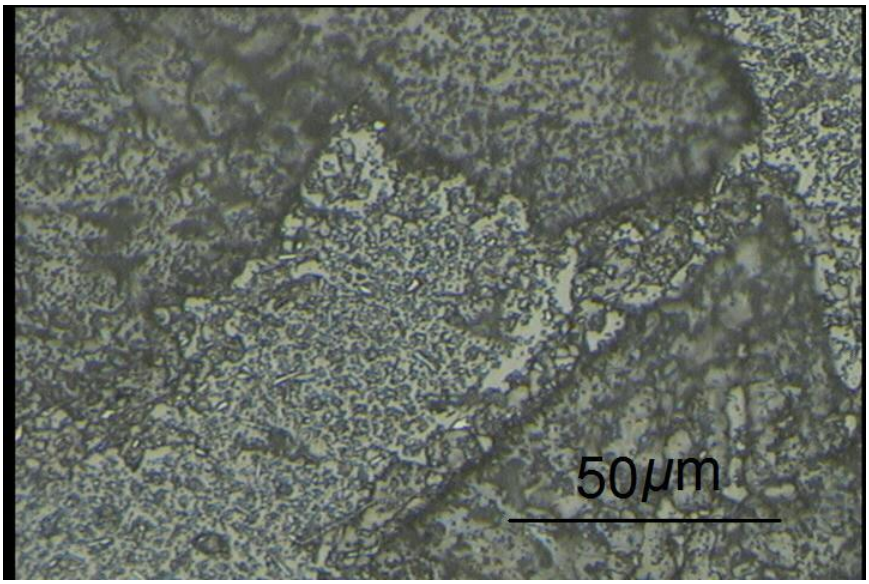

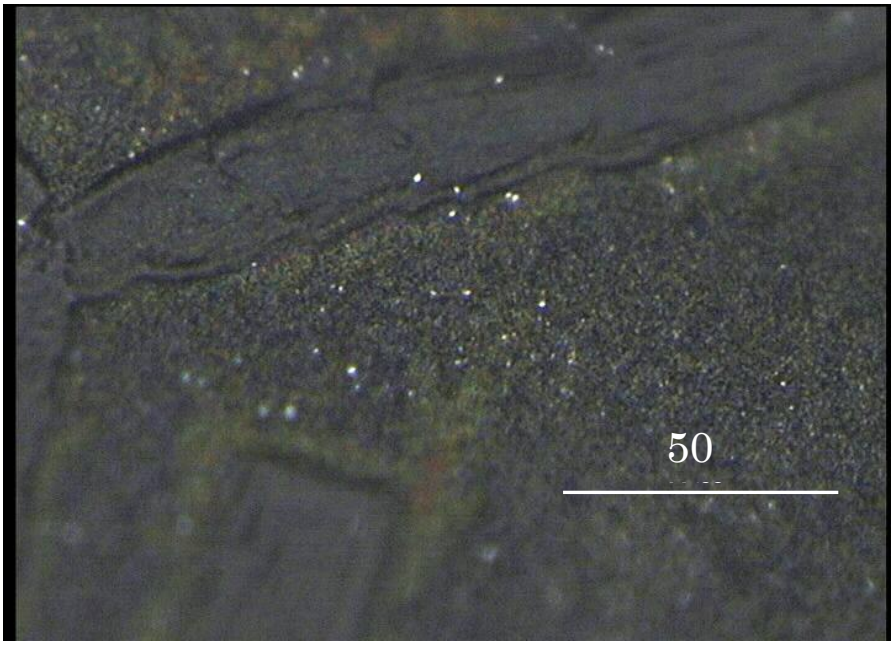

Fig. 3.12 Optical microscopic photographs of the Ag-deposited electrode surface in (A) 25 mM $AgNO_3$ + 1 M KNO_3 + 9 g dm^{-3} sodium alginate, (B) 25 mM $AgNO_3$ + 1 M KNO_3 solutions, and (C) 12.5 mM $AgNO_3$ + 1 M KNO_3 solution.

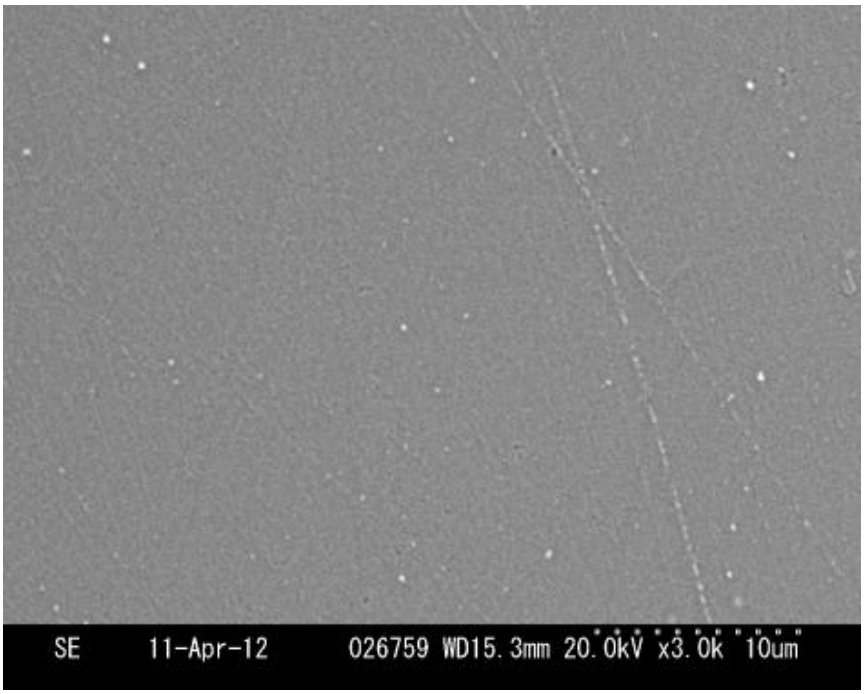

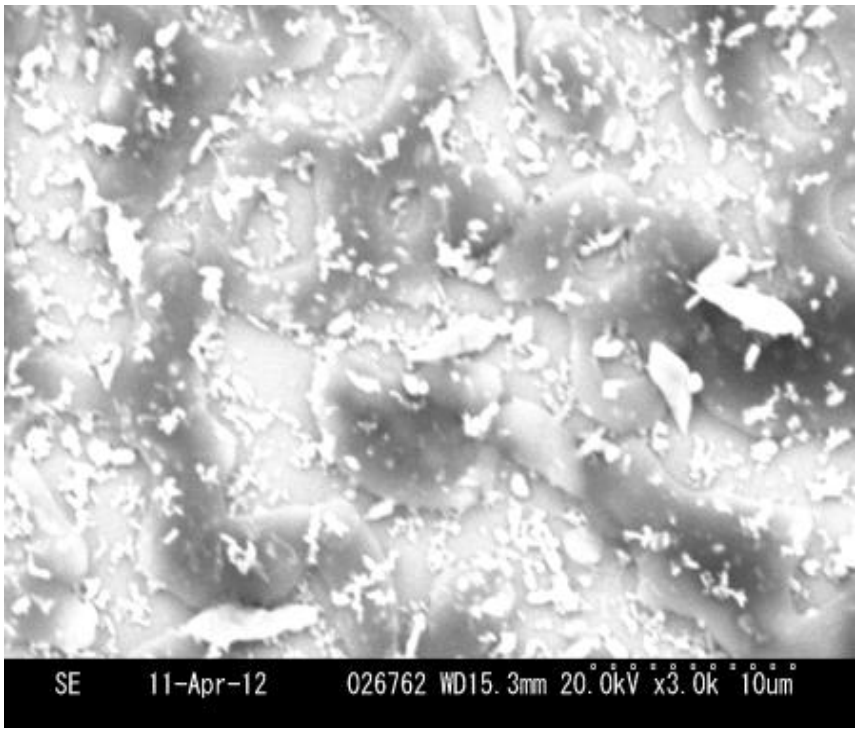

Fig. 3.13 SEM photographs of the Ag-deposited electrode surface in (A) 25 mM $AgNO_3$ + 1 M KNO_3 + 9 g dm^{-3} sodium alginate and (B) 25 mM $AgNO_3$ + 1 M KNO_3 solutions.

3.3 Conclusions

With an increase in concentrations of sodium alginate, the viscosity of ionic solution increases up to actually solid states. Diffusion coefficients of ions, however, do not vary with the viscosity as if the ions were in water. The value of the intrinsic viscosity is so large that one mole of the unit of sodium alginate polymer can make 3 m^3 aqueous solution viscous. Consequently ions diffuse in the domain of the aqueous solution without collision with the network of sodium alginate. Sodium alginate is extremely efficient in generating viscosity.

Sodium alginate solution is useful to keep ideal concentration profiles by diffusion

long (a half hour) without effects of natural convection and/or of stray vibrations. The property of retaining ideal mass transport can be applied to metal plating. The silver metal cathodically deposited in sodium alginate solution has no morphology.

3.4 References

[1] A. Haug, B. Larsen, O. Smidsrod, Acta Chem. Scand. 20 (1966) 183.

[2] Z.Y. Wang, Q. Z. Zhang, M. Konno, S. Saito, Biopolym. 34 (1994) 737.

[3] A. Regand, H.D. Goff, Food Hydrocolloids 17 (2003) 95.

[4] C.-C. Wu, H.-N. Luk, Y.-T. T. Lin, C.-Y. Yuan, Talanta 81 (2010) 228.

[5] A. Kikuchi, M. Kawabuchi, A. Watanabe, M. Sugihara, Y. Sakurai, T. Okano, J. Control. Rel. 58 (1999) 21.

[6] G. Zhao, X. Zhan, W. Dou, Anal. Biochem. 408 (2011) 53.

[7] A.C.F. Ribeiro, A.J.F.N. Sobral, S.M.N. Simoes, M.C.F. Barros, V.M.M. Lobo, A. M.T.D.P.V. Cabral, F.J.B. Veiga, C.I.A.V. Santos, M.A. Esteso, Food Chem. 125 (2011) 1213.

[8] S. Wei, W. Dandan, G. Ruifang, J. Kui, Electrochem. Commun. 9 (2007) 1159.

[9] T. Zhan, M. Xi, Y. Wang, W. Sun, W. Hou, J. Colloid Interface Sci. 346 (2010) 188.

[10] X. Wang, M. Han, J. Bao, W. Tu, Z. Dai, Anal. Chim. Acta 717 (2012) 61.

[11] Y. Hu, N. Hu, J. Phys. Chem. B 112 (2008) 9523.

[12] U.S. Toti, T.M. Aminabhavi, J. Membr. Sci. 228 (2004) 199.

[13] M. Grassi, I. Colombo, R. Lapasin, J. Control. Rel. 76 (2001) 93.

[14] W. Lubas, P. Ander, Macromolecules 13 (1980) 318.

[15] Y. Li, X. Zhao, Q. Xu, Q. Zhang, D. Chen, Langmuir 27 (2011) 6458.

[16] A. Mohanan, B. Vishalakshi, Int. J. Polym. Mat. 58 (2009) 561.

[17] A.R. Kulkarni, K.S. Soppimath, T.M. Aminabhavi, W.E. Rudzinski, Eur. J. Pharm. Biopharm. 51 (2001) 127.

[18] D. Şolpan, M. Torun, J. Appl. Polym. Sci. 100(2006) 335.

[19] H. Zhou, S. Dong, Electrochim. Acta 42 (1997) 1801.

[20] H. Zhou, N. Gu, S. Dong, J. Electroanal. Chem. 441 (1998) 153.

[21] I. Svorstøl, T. Sigvartsen, J. Songstad, J. Acta Chem. Scand. B42 (1988) 133.

[22] R.A. Mashelkar, A. Dutta, Chem. Eng. Sci. 37 (1982) 969.

[23] J. Legrand, E. Dumont, J. Comiti, F. Fayolle, Electrochim. Acta 45 (2000) 1791.

[24] K. Aoki, K. Tokuda, H. Matsuda, N. Oyama, J. Electroanal. Chem. 176 (1984) 139.

[25] P. Daum, J. R. Lenhard, D. Rolison, R. W. Murray, J. Am. Chem. Soc. 102 (1980) 4649.

[26] P. Zuman, D. Rozbroj, J. Ludvík, M. Aleksic, L. Camaione, H. Celik, J. Electroanal. Chem. 553 (2003) 135.

[27] K. Aoki, Y. Guo, J. Chen, J. Electroanal. Chem. 629 (2009) 73.

[28] Y. Guo, K. Aoki, J. Chen, T. Nishiumi, Electrochem. Acta, 56 (2011) 3727.

[29] P.W. Atkins, Physical Chemistry, Sixth edition, Oxford University Press, Oxford, 1998, p. 479

[30] K. Aoki, K. Akimoto, K. Tokuda, H. Matsuda, J. Osteryoung, J. Electroanal. Chem. 171 (1984) 219.

[31] P.W. Atkins, Physical Chemistry, Sixth edition, Oxford University Press, Oxford, 1998, pp. 690-691.

[32] H.A. Latinen, Trans. Electrochem. Soc. 82 (1942) 289.

[33] A. J. Bard, L.R. Faulkner, Electrochemical Methods, Fundamentals and Applications, Second edition, 2001, John Wiley & Sons, New York. p. 163.

Slow scan voltammetry for diffusion-controlled currents in sodium alginate solutions

4.1 Aim

Voltammetry at slow scan rates less than 0.1 mV s^{-1} is useful for exhibiting well-defined redox responses in searching for performance of lithium ion batteries [1]. The voltammetric peak currents were controlled by diffusion of lithium in graphite, as was demonstrated by the proportionality of the currents to square-roots of scan rates [21]. The controlling step was also supported by the Cottrell plot for long-term chronoamperometric responses of reduction of lithium ions [2]. The voltammetric capacitive current is, in contrast, proportional to the scan rate. If observed current is a simple sum of the diffusion-controlled current, I_d, and the capacitive one, I_c, the ratio, I_c/I_d, decreases by 10 times with 100 times decrease in the scan rates. This is a reason for exhibiting the advantage of extremely slow scan voltammetry. A key of obtaining slow scan voltammograms reproducibly is to prevent disturbance from natural convection at a long term measurement. Fortunately, the current by the intercalation is controlled by diffusion of metal atoms into solid anodes [21,3-5] and solid cathodes [6-9], and hence disturbance by convection ought to be suppressed. This advantage has been realized also in voltammetry at film-coated electrodes in a thin layer cell [10-16]. Natural convection may be mechanically suppressed not only with the viscous films but also with the film boundary. Slow scan voltammetry has also been applied to detection of catalytic currents [17-21] at the aim of enhancing catalytic kinetics over mass transport. It has been used for obtaining well-defined voltammograms at low temperatures [22].

In order to apply slow scan voltammetry to general usage without the above limited conditions of electrolysis, it is necessary to avoid unexpected natural convention or mass transport of products generated at a counter electrode to the working electrode. A technique of preventing natural convection is to use viscous solvents [23-31]. An

increase in the viscosity decreases generally the diffusion coefficient, according to the Stokes-Einstein equation [32], so that Faradaic currents also decrease. Addition of sodium alginate (SA) enhances the viscosity without changing diffusion coefficients of molecules [44,46,33-36]. Molecules may not collide with the network of SA but diffuse through the domain of the aqueous solution [56]. Consequently slow scan voltammetry in SA may exhibit a potentiality of extracting Faradaic currents from capacitive ones.

The other technique of extracting Faradaic currents from background currents is microelectrode voltammetry. Unfortunately, microdisk electrodes are unsuitable for detecting low concentrations of electroactive species because of difficulty in detecting very small current. Microdisk array electrodes and microband electrodes have large surface area. However, they also have long boundaries between the electrode and the insulating wall, which yields large irreproducible capacitive current. It is a long cylindrical or a long wire electrode that shows large currents under quasi steady-state current [37,38]. A wire electrode has another advantage of yielding reproducible Faradaic currents, because the boundary between the wire and the insulator which often causes floating capacitive currents is much shorter than the length of the wire [39,40]. If wire electrodes are used in SA solution at slow scans, they are expected to show highly sensitive Faradaic currents with negligible effects of natural convention.

This report deals with finding practical conditions of exhibiting diffusion-controlled voltammograms at slow scans in aqueous solutions. Aminoferrocene and hexacyanoferrate are used for redox species in SA solution which suppresses natural convection during long term electrolysis. A disk electrode and a long wire electrode are employed for determining the lowest limit of the concentrations.

4.2 Results and Discussion

Figure 4.1 shows linear sweep voltammograms of $Fe(CN)_6^{4-}$ in KCl solution (A)

without and (B) with SA at the platinum electrode 1.6 mm in diameter at low scan rates. Voltammograms at scan rates, *v*, over 5 mV s^{-1} exhibited conventional, peaked currents (not shown), similar to those in Fig. 4.1(B). Voltammograms of FcTMA were close to those in Fig.4.1 except for peak potentials and the sign of waves. Voltammograms of both $Fe(CN)_6^{4-}$ and FcTMA without SA showed complicatedly wave-like variations at *v* < 0.5 mV s^{-1} (Fig. 4.1(A)). The complication is probably due to natural convection. When SA was added to the solution so that the viscosity increased by 50 times, the voltammetric currents were slightly smaller than those without SA. According to Randles-Sevcik's equation, the decrease in the diffusion coefficient by 50 times should decrease the peak current by 7 times. The small difference in the peak currents with and without SA has been explained in terms of the easy permeation of redox species through the network structure of SA [56]. Since SA molecules include carboxylic groups, they may form complexes with cations, as for silver ion [56]. No complication for FcTMA was found, for example, precipitation and shift of the oxidation potential. No redox reaction of SA was found in the SA solution without redox species, as shown by the dashed curve in Fig. 4.1B.

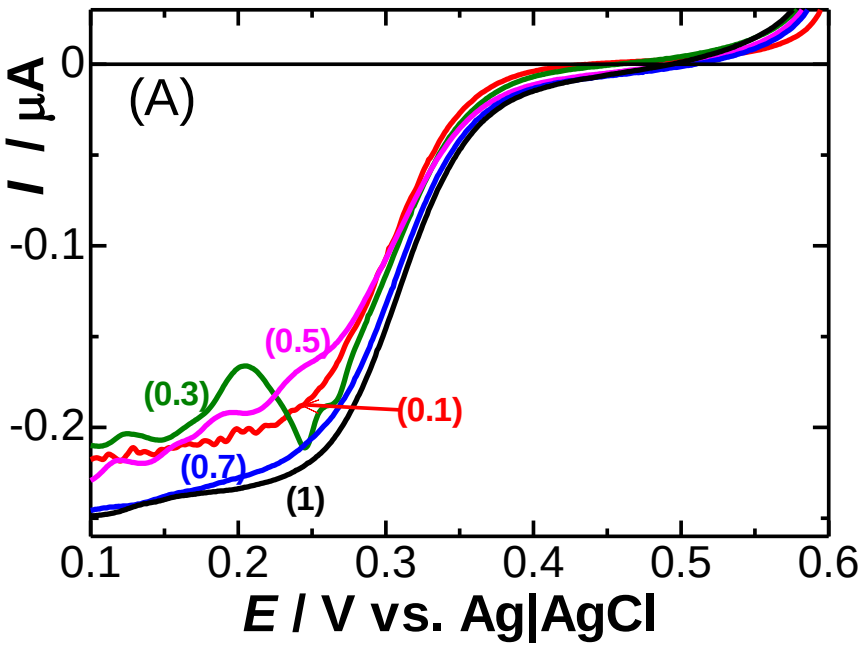

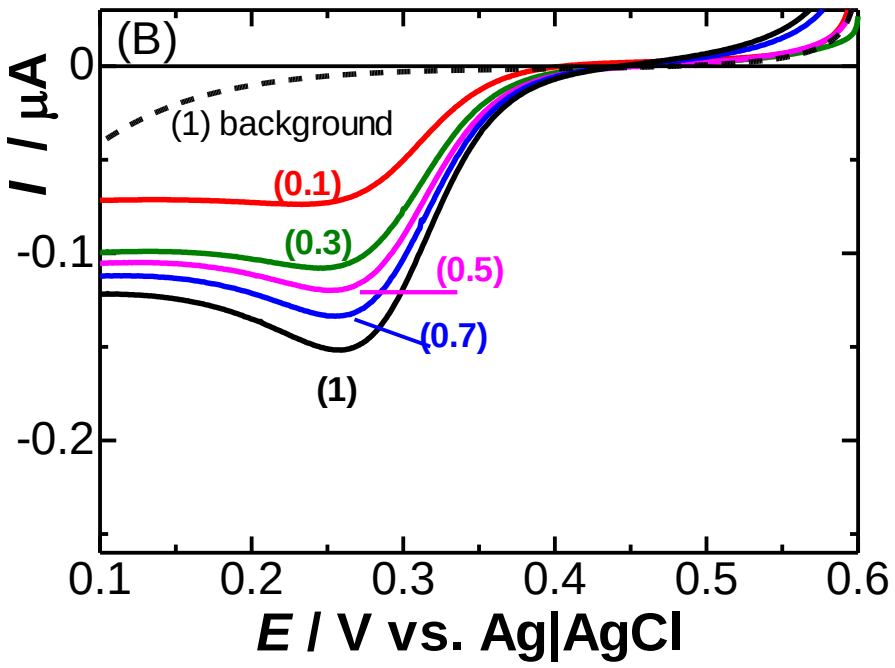

Figure 4.1. Linear sweep voltammograms of 0.25 mM $Fe(CM)_6^{4-}$ in (A) 0.5 M KCl aqueous solution and (B) solution (A) + 12 mg cm^{-3} SA at the platinum disk electrode 1.6 mm in diameter. The indicated numbers are scan rates in mV s^{-1} unit. The dashed curve is the background current of SA solution at 1 mV s^{-1}.

Figure 4.2 shows dependence of the peak currents of FcTMA and $Fe(CN)_6^{4-}$ with (triangles) and without (circles) SA on $v^{1/2}$. The peak currents with SA for v > 3 mV s^{-1} were almost the same as those without SA, whereas those with SA for v < 1 mV s^{-1} were smaller than those without SA. The ratio of the peak currents with SA, $|I_p|_{SA}$, to that without SA, I_p, is plotted against $v^{1/2}$ on the right ordinate in Fig.4.2 The deviation of $I_p/|I_p|_{SA}$ from unity increases with a decrease in the scan rates. The increase must be due to natural convection by taking into account of Fig.4.1 (A). The fact of $|I_p|_{SA} = I_p$ for v > 3 mV s^{-1} suggests no adsorption of SA on the electrode.

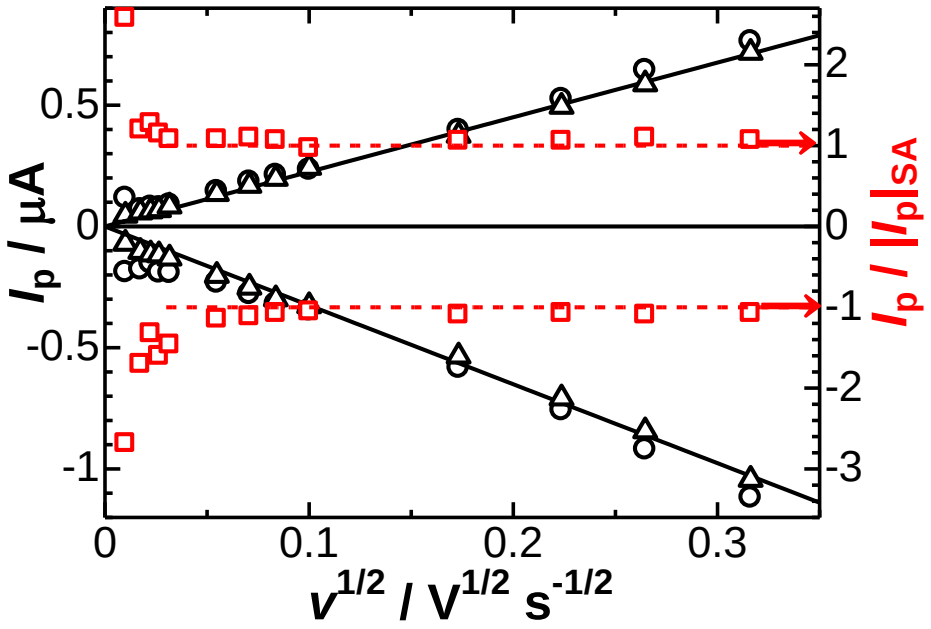

Figure 4.2 Plots of peak currents (triangles) with and (circles) without SA at the disk electrode against the square-roots of the scan rates on the left ordinate. The ratio of the currents is plotted on the right ordinate.

The currents in SA solutions for $v > 3$ mV s^{-1} in Fig.4.2 were accurately proportional to $v^{1/2}$, whereas those for $v < 3$ mV s^{-1} deviated from the proportionality. The deviation is ascribed to the edge effect of diffusion [41], because the peak current for small values of $a(Fv/RTD)^{1/2}$ is approximated as

$$I_p \approx 0.446AFc^* \sqrt{FDv/RT} + 2.1Fc^*Da \qquad (4.1)$$

where a is the radius of the disk electrode and D is the diffusion coefficient of the electroactive species. Therefore, slow scan voltammograms include currents with the edge effect of diffusion even at a large disk electrode. The voltammograms without SA deviate from the proportionality for $v < 5$ mV s^{-1} more largely than those with SA.

The platinum wire 0.1 mm in diameter and 10 mm in length was used as a working electrode. The length was the immersing distance rather than that provided by an insulator. The wave form of linear sweep voltammograms was sigmoid at low scan rates, and had peaked shape at fast scans. The voltammograms of FcTMA without SA at $v < 1$ mV s^{-1} contained irregular waves or noises, as shown in Fig. 4.3(a). In contrast, a voltammogram with SA showed a smooth curve with a vague peak (Fig. 4.3(b)). The peak currents or the limiting currents with SA were larger than those without SA.

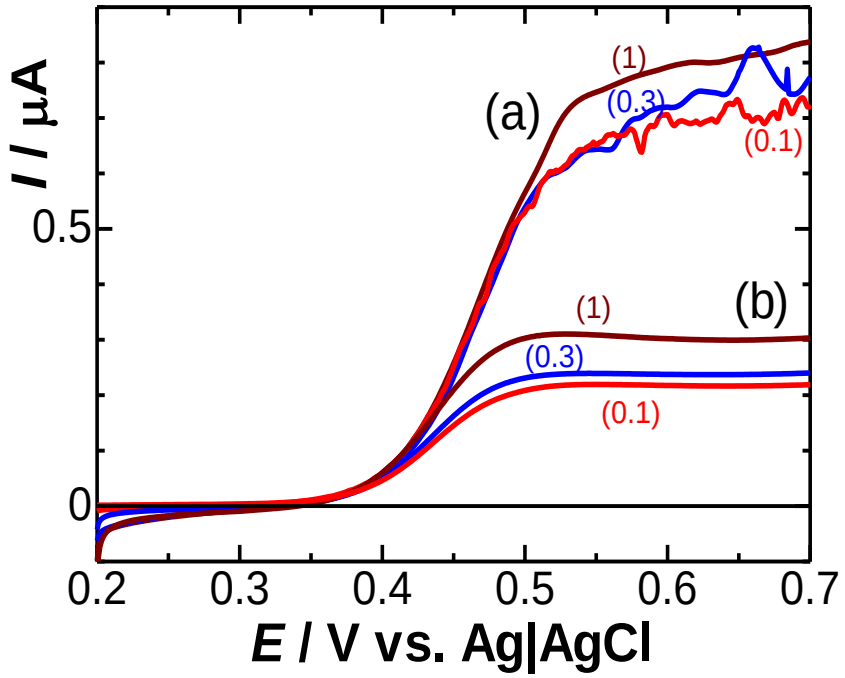

Figure 4.3. Linear sweep voltammograms of 0.25 mM FcTMA in 0.5 M KCl aqueous solution (a) without and (b) with SA (43 mPa s) at the wire electrode 0.1 mm in diameter and 10 mm in length. The indicated numbers are scan rates in mV s^{-1} unit.

Peak currents or limiting currents, I_L, for $Fe(CN)_6^{4-}$ ($I_L < 0$) and FcTMA ($I_L > 0$) were obtained at various scan rates, and were plotted against $v^{1/2}$ in Fig.4.4. The currents with SA had a linear relationship with $v^{1/2}$ rather than a proportional relation. Appearance of the intercept can be predicted from the theoretical expression for cylindrical diffusion [42]. The current ratio for $v < 50$ mV s^{-1}, plotted on the right ordinate in Fig.4.4, was larger than unity. The ratio of the currents for $v > 20$ mV s^{-1} in Fig. 4.4 (the wire) is larger than that in Fig. 4.2 (the disk). Wire electrodes are more strongly affected by natural convection than disk electrodes at slow scans. Noiseless voltammograms in SA solution (in Fig. 3(b)) indicates that SA suppresses convection at wire electrodes.

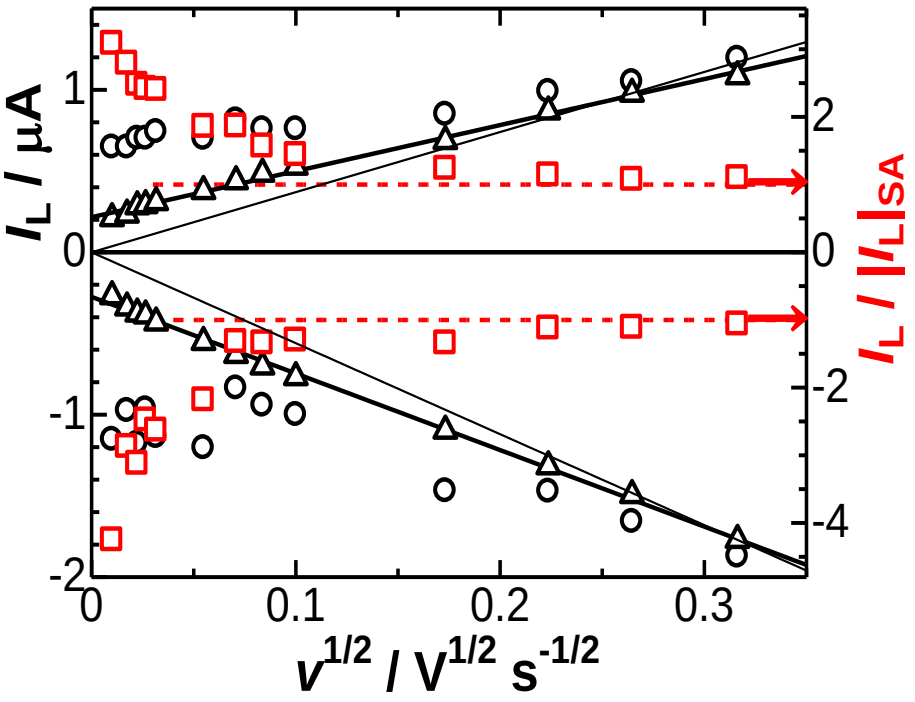

Figure 4.4 Plots of peak currents (triangles) with and (circles) without SA at the wire electrode against the square-roots of the scan rates on the left ordinate. The ratio of the currents is plotted on the right ordinate.

In order to see fluctuation of the current by natural convection, we made long-term chronoamperometry at 0.55 V for FcTMA and 0.15 V for $Fe(CN)_6^{4-}$. Figure 4.5 shows chronoamperometric curves at the (A) disk and (B) wire electrode in solutions (a, c) with and (b, d) without SA, where $I > 0$ is for FcTMA and $I < 0$ is for $Fe(CN)_6^{4-}$.

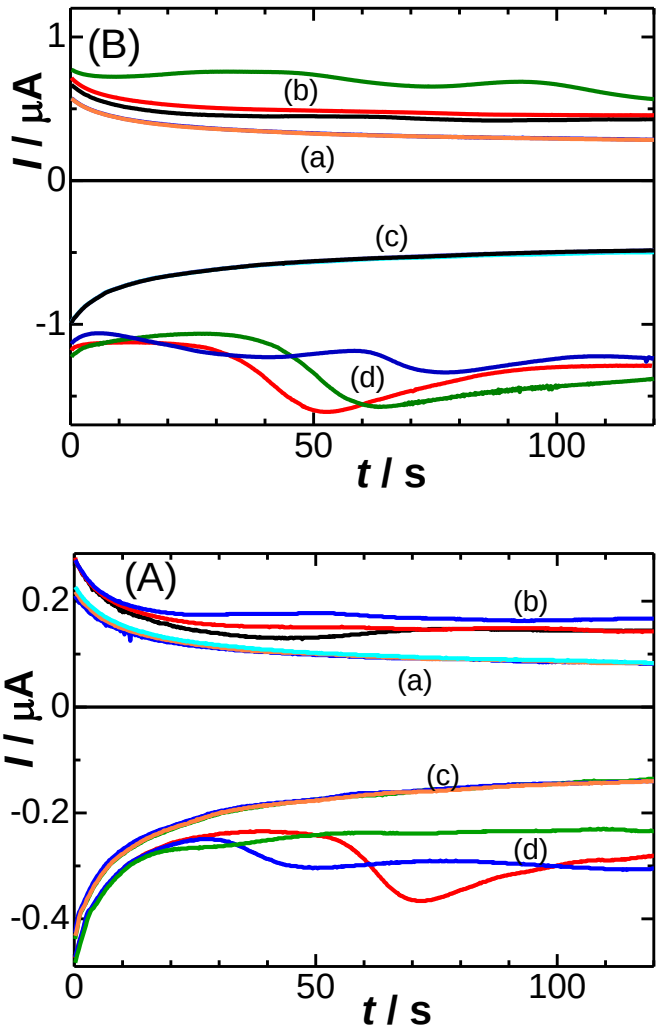

Figure 4.5 Chronoamperometric currents of 0.25 mM FcTMA and 0.25 mM $Fe(CN)_6^{4-}$ in 0.5 M KCl when the potentials 0.55 V (FcTMA) and 0.15 V ($Fe(CN)_6^{4-}$) were applied to (A) the disk electrode and (B) the wire electrode. Curves (a) and (c) are for solution with SA, while those of (b) and (d) are for solution without SA.

Three current-time curves with SA (a, c) were overlapped each other. Curves without SA varied from run to run at times over 10 s, and their currents, $|I|$, were larger than $|I|_{SA}$. Irreproducibility of the currents at the wire electrode (B) was noticeable earlier than that at the disk electrode (A).

Slow scan voltammetry in the SA solution is expected to discern low concentrations of electroactive species from capacitive currents. We obtained voltammograms of 1 μM FcTMA at various slow scan rates, as shown in Fig. 4.6 (A) without and (B) with SA. When solution contained SA, the faradaic waves were obtained clearly and reproducibly even at v = 0.01 mV s^{-1}. The background-corrected limiting currents of 1 μM FcTMA in the SA solution are plotted against $v^{1/2}$ in Fig.4.7. Fluctuation was small enough for determining the limiting currents. The linear dependence of the current on $v^{1/2}$ was close to that in Fig. 4.4.

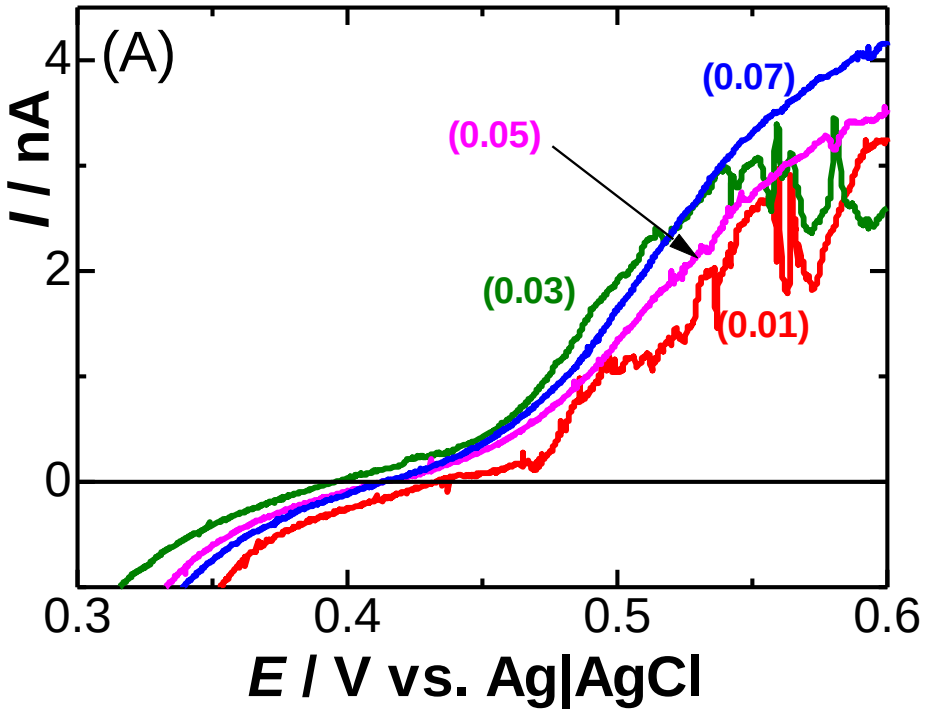

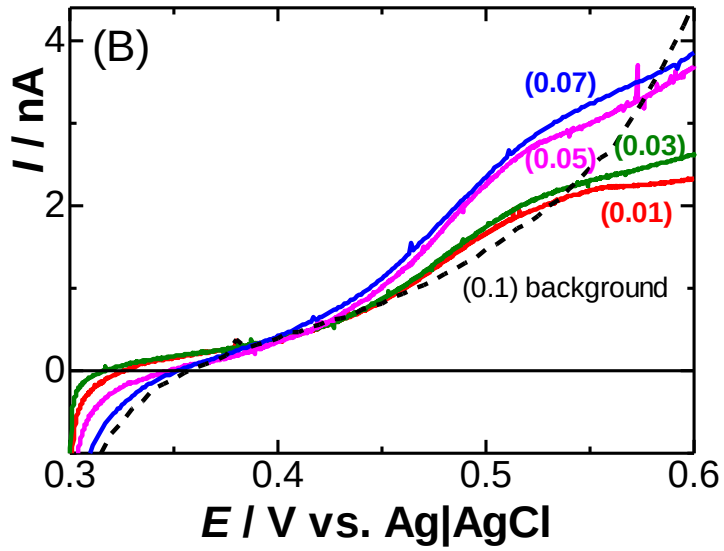

Figure 4.6 Linear sweep voltammograms of 1 μM FcTMA in 0.5 M KCl aqueous solution (A) without and (B) with SA (43 mPa s) at the wire electrode 0.1 mm in diameter and 10 mm in length for the indicated scan rates in mV s^{-1}. The dashed curve is the background current of SA solution at 0.1 mV s^{-1}.

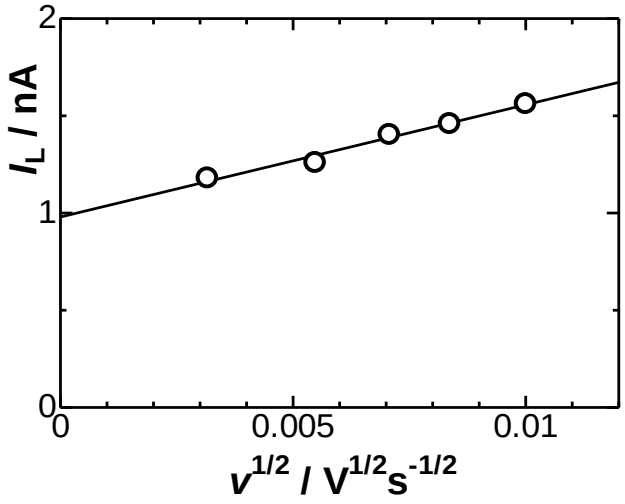

Figure 4.7 Plot of the background-corrected limiting currents of 1 μM FcTMA in 0.5 M KCl + SA solution against $v^{1/2}$.

Analytical significance of voltammograms is not only well-defined, reproducible waveform but also proportionality of the current to concentration. We examined whether limiting currents of background-corrected, reproducible voltammograms were proportional to concentrations at several scan rates. The limiting currents are plotted against concentrations of FcTMA for two scan rates in Fig.4.8, where slopes of the solid lines are unity. The lowest concentration at v = 100 mV s^{-1} in the viewpoints of background correction and reproducibility was 0.01 mM, regardless of the presence or the absence of SA. Experimental values fell on a dashed line with a slope smaller than unity (in Fig. 8), probably because of a contribution of capacitive currents at low concentrations. In contrast, the slow scan of 0.1 mV s^{-1} allowed us to obtain the reliable limiting current up to 1 μM without SA. When solutions contained SA, the readily available lowest concentration was 0.5 μM.

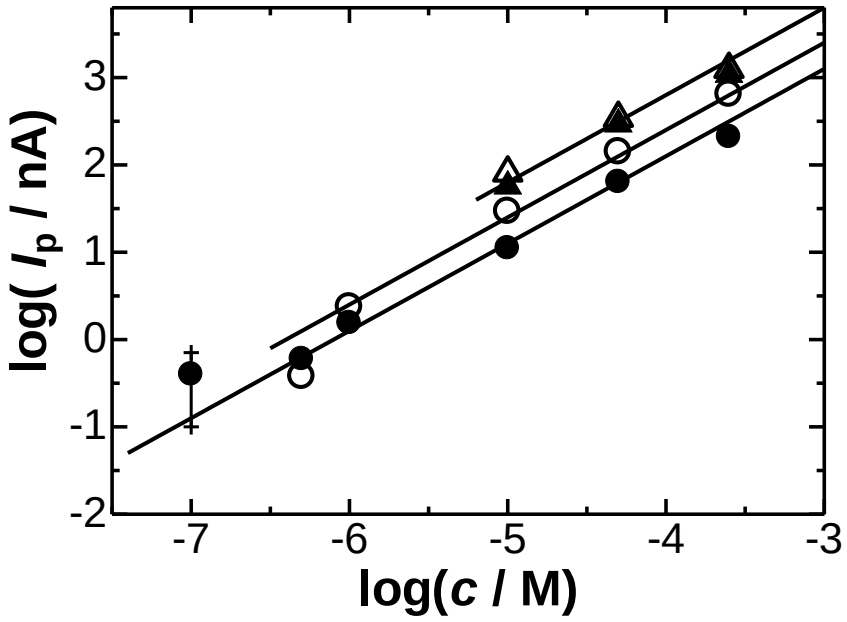

Figure 4.8 Logarithmic variations of the limiting currents with concentrations of FcTMA in 0.5 M KCl solutions with (filled marks) and without (open marks) SA at the wire platinum electrode for v = (triangle) 100 and (circles) 0.1 mV s^{-1}.

4.3 Conclusions

Slow scan voltammetry is quantitatively demonstrated to discern diffusion-controlled current from capacitive one. The reason of the successful discrimination is the difference in scan rate dependence of the two currents. Slow scan voltammograms are necessarily complicated by uncontrollable natural convention. The convection can be suppressed with addition of SA, which decreases viscosity tremendously but does not alter diffusion coefficients of redox species. Therefore voltammograms can be obtained reproducibly without blocking redox reactions. Slow scan voltammetry can be used as a conventionally electrochemical tool if SA is added to solution.

Slow scan voltammetry is suitable for detection of redox species with low concentrations. Recommended electrodes for this purpose are wire electrodes without shielding by insulating wall, because shielding is a source of large and irreproducible capacitive currents. Although a wire electrode is normally unsuitable for long electrolysis owing to fluctuation by convection, addition of SA to solutions can keep quasi-state state currents reproducible. Voltammetry for ν = 0.1 mV s^{-1} at a wire electrode in SA solution allows us to determine concentrations up to 0.5 μM without specific instrumentation. However, long time is consumed. As a conclusion, an advantage of the present technique is determination of concentration without effects of adsorption of redox species and capacitive currents because of long time electrolysis.

4.4 References

[1] M.D. Levi, D. Aurbach, J. Electroanal. Chem. 421 (1997) 79.

[2] M.D. Levi, E.A. Levi, D. Aurbach, J. Electroanal. Chem. 421 (1997) 89.

[3] M. Minakshi, Electrochim. Acta 55 (2010) 9174.

[4] T. Ohzuku, Y. Iwakoshi, K. Sawai J. Electrochem. Soc. 140 (1993) 2490.

[5] F. Nobili, S. Dsoke, M. Mancini, R. Tossici, R. Marassi, J. Power Sources 180 (2008) 845.

[6] J.-H. Kim, K. Zhu, J. Y. Kim, A. J. Frank, Electrochim. Acta 88 (2013) 123.

[7] Z. Lu, M.D. Levi, G. Salitra, Y. Gofer, E. Levi, D. Aurbach, J. Electroanal. Chem. 491 (2000) 211.

[8] M. Liberatore, F. Decker, A. S. Vuk, B. Orel, G. Drazic, Solar Energy Mat. 90 (2006) 434.

[9] K.M. Begam, Y.H. Taufiq-Yap, M.S. Michael, S.R.S. Prabaharan, Solid State Ionics 172 (2004) 47.

[10] C. Shi, F. C. Anson, Anal. Chem. 70 (1998) 3114.

[11] C. Shi, F. C. Anson, J. Phys. Chem. B 103 (1999) 6283.

[12] M. Liberatore, A. Petrocco, F. Caprioli, C. La Mesa, F. Decker, C.A. Bignozzi, Electrochim. Acta 55 (2010) 4025.

[13] T.D. Chung, J. Kor. Electrochem. Soc. 5 (2002) 216.

[14] F. Quentel, V. Mirceski, M. L'Her, F. Spasovski, M. Gacina, Electrochem. Commn. 9 (2007) 2489.

[15] V. Mirceski, R. Gulaboski, I. Bogeski, M. Hoth, J. Phys. Chem. C 111 (200) 6068.

[16] X. Liu, L. Hu, L. Zhang, H. Liu, X. Lu, Electrochim. Acta 51 (2005) 467.

[17] F. Maillard, M. Martin, F. Gloaguen, J.-M. Leger, Electrochim. Acta 47 (2002) 3431.

[18] Y. Liu, S. Mitsushima, K. Ota, N. Kamiya, Electrochim. Acta 51 (2006) 6503.

[19] F. Seland, R. Tunold, D. A. Harrington, Electrochim. Acta 55 (2010) 3384.

[20] M. Yagi, K. Nagai, T. Onikubo, M. Kaneko, J. Electroanal. Chem. 383 (1995) 61.

[21] A.D. Modestov, M.R. Tarasevich, H. Pu, J. Power Sources 205 (2012) 207.

[22] M. Opallo, J. Electroanal. Chem. 411 (1996) 145.

[23] C.-C. Wu, H.-N. Luk, Y.-T. T. Lin, C.-Y. Yuan, Talanta 81 (2010) 228.

[24] A. Kikuchi, M. Kawabuchi, A. Watanabe, M. Sugihara, Y. Sakurai, T. Okano, J. Control. Rel. 58 (1999) 21.

[25] G. Zhao, X. Zhan, W. Dou, Anal. Biochem. 408 (2011) 53.

[26] A.C.F. Ribeiro, A.J.F.N. Sobral, S.M.N. Simoes, M.C.F. Barros, V.M.M. Lobo, A. M.T.D.P.V. Cabral, F.J.B. Veiga, C.I.A.V. Santos, M.A. Esteso, Food Chem. 125 (2011) 1213.

[27] K. Aoki, Y. Guo, J. Chen, J. Electroanal. Chem, 629 (2009) 73.

[28] Y. Guo, K. Aoki, J. Chen, T. Nishiumi, Electrochem. Acta, 56 (2011) 3727.

[29] J. Legrand, E. Dumont, J. Comiti, F. Fayolle, Electrochim. Acta 45 (2000) 1791.

[30] R. D. Tonini, M. R. Remorino, F. M. Brea, Electrochim. Acta, 23 (1978) 699.

[31] J. van der Gucht, N. A. M. Besseling, H. P. van Leeuwen, J. Phys. Chem. B 108 (2004) 2531.

[32] P.W. Atkins, Physical Chemistry, Sixth edition, Oxford University Press, Oxford, 1998, pp. 690-691.

[33] M. Grassi, I. Colombo, R. Lapasin, J. Control. Rel. 76 (2001) 93.

[34] W. Lubas, P. Ander, Macromolecules 13 (1980) 318.

[35] Y. Li, X. Zhao, Q. Xu, Q. Zhang, D. Chen, Langmuir 27 (2011) 6458.

[36] K. Aoki, B. Wang, J. Chen, T. Nishiumi, Electrochim. Acta, 83 (2012) 348.

[37] K. Aoki, K. Honda, K. Tokuda, H. Matsuda, J. Electroanal. Chem. 182 (1985) 267.

[38] K. Aoki, Electroanalysis 5 (1993) 627.

[39] K. Aoki, Y. Hou, J. Chen, T. Nishiumi, J. Electroanal. Chem. 689 (2013) 124.

[40] K. Aoki, X. Zhao, J. Chen, T. Nishiumi, J. Electroanal. Chem. 697 (2013) 5.

[41] K. Aoki, K. Akimoto, K. Tokuda, H. Matsuda, J. Osteryoung, J. Electroanal. Chem.

171 (1984) 219.

[42] K. Aoki, K. Aikimoto, K. Tokuda, H. Matsuda, J. Osteryoung, J. Electroanal. Chem. 182 (1985) 267.

Conclusions

Voltammetry current was examined in different concentrations by use of ferrocenyl derivate (FcMA) as redox species. Voltammograms were almost independent of the increasing viscosity of the SA solution even in a solid-like state. The diffusion coefficient of the FcTMA did not vary with the viscosity evaluated by a viscometer. The conductivity was not only independent of *D* but also of redox species. The independence was confirmed by means of time-evolution of diffusing dye experiment. The result showed the *D*-values were close to the value of organic molecular in water regardless of the viscosity. The intrinsic viscosity was evaluated. The value 15 dm^3g^{-1} equivalent to the volume as large as $3m^3$ of water in which one mole of the unit of SA polymer generates the viscosity. In contrast, diffusion coefficients of the latex particle which was 0.84 μm and 0.42μm in diameter by DLS and Stokes-Einstein equation respectively, decreased with the increasing of the viscosity of SA. It demonstrated molecules bigger than that volume would exhibit viscous effects by blocking diffusion with the network of SA. As an application, it can use for long long-term chronoamperometry experiments. The reproducible current of different angle of electrode surface against the horizon (0, 60) got with the time even of 1500s without any effect of nature convection, whereas it was irreproducible for times longer than 20s. The silver film deposited in SA solution exhibited no morphology even on an optical microscopy scale.

The linear sweep voltammograms of two redox species, FcTMA and potassium hexacyanoferrate in KCl solution with SA at platinum disc electrode were clear , reproducible and propotional to the square root of scan rate, whereas that in aqueous solution were complicatedly wave-like variations at lower scan rate. The peak currents with SA were almost the same as those without SA, whereas they were smaller than those without SA at low scan rate. The ratio of the peak currents with SA to that without

SA was increased with decreasing of scan rate. The similar variation of voltammograms and peak current happened at platinum wire electrode 0.1mm in diameter and 10mm in length, but a wire electrode were more strongly affected by natural convection than a disc electrode at low scan rate. Irreproducible and larger chronoamperometric currents at the wire electrode were noticeable earlier than that at the disk electrode. Slow scan voltammetry is suitable for detection of redox species with low concentrations. A wire electrode in SA solution was demonstrated to be a powerful tool for determining concentrations up to 0.5μM at 0.1 mV s^{-1}. The faradaic current waves were obtained clearly and reproducibly even at 0.01 mV s^{-1}.